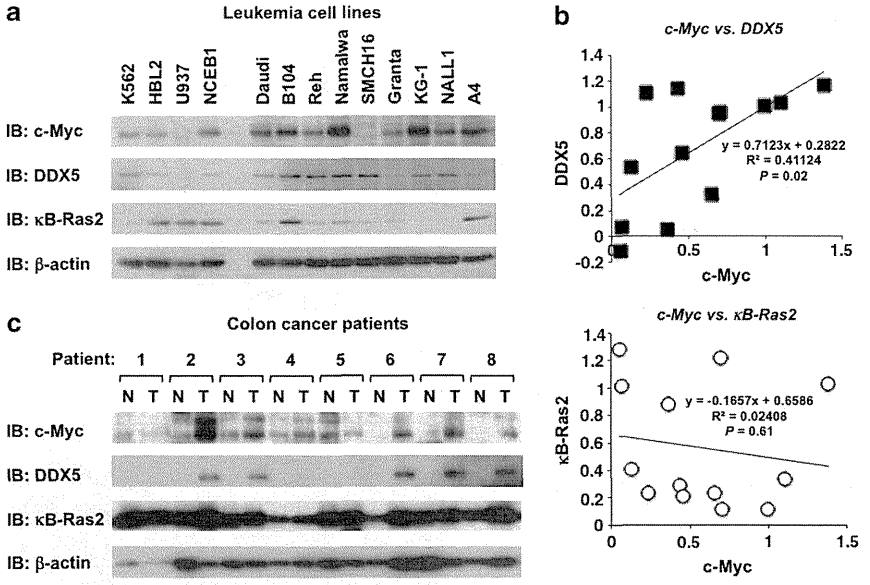

Figure 7. Correlative expressions of c-Myc and DDX5 in leukemia and colon cancers. Expression levels of c-Myc, DDX5, κB-Ras2 and β-actin were analyzed by immunoblotting. The results from the samples of leukemia cell lines are shown in **a**. (**b**) Shows the correlation between the expressions of c-Myc and DDX5, or c-Myc and κB-Ras2 in the graph. As a result, c-Myc and DDX5 showed an intermediate positive correlation. The results of immunoblot analysis of lysates from normal tissues (N) and colon cancer (T) are shown in **c**.

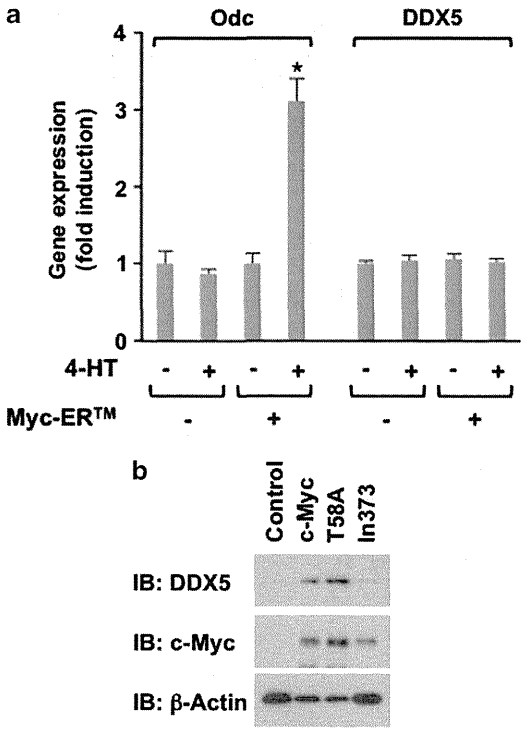

Figure 8. *DDX5* is not a target gene of c-Myc. (**a**) NIH-3T3 cells infected with retroviruses harboring Myc-ER were treated with 1 μM 4-HT and 12 h later, total RNA was prepared and used for quantitative PCR for Odc and DDX5. (**b**) TKO MEFs were infected with the retroviruses harboring wild-type c-Myc, T58A mutant and In373 mutant, respectively. After puromycin selection for 3 days, the cell lysates were prepared, and analyzed by immunoblotting with anti-DDX5, anti-c-Myc and anti-β-actin antibodies, respectively. Error bars mean s.d. ($n = 3$, $^*P < 0.01$).

expression of DDX5 was analyzed.[35,36] As shown in Figure 8b, wild-type c-Myc and T58A mutant effectively increased the DDX5 expression, whereas In373 mutant showed little effect, suggesting that DNA-binding activity of c-Myc is required for the induction of DDX5 expression. Therefore, we next labeled TKO cells with [^{35}S] methionine to analyze the effect of c-Myc on the protein synthesis and degradation of DDX5 (Figure 9a). As shown in Figures 9b and c, c-Myc drastically affected the rate of protein synthesis of DDX5 rather than its degradation. Furthermore, the enforced expression of Arf clearly canceled the c-Myc-induced acceleration of protein synthesis of DDX5 (Figure 9d). These findings strongly suggest that c-Myc results in high expression of DDX5 in tumor cells through the acceleration of protein synthesis of DDX5, and Arf impedes this in a p53-independent manner.

DISCUSSION

The present findings suggest the critical roles of DDX5 in mediating Arf-induced, p53-independent cell proliferation arrest, and the direct feedback mechanism between DDX5 and Arf provided here would play an indispensable role in novel p53-independent checkpoint preventing c-Myc-mediated tumorigenesis by Arf (Figure 10).

As Arf binds to the catalytic domain of DDX5, Arf is supposed to block the activity of DDX5 directly (Figure 2b). Furthermore, we also found that induced expression of Arf caused the nucleolar localization of DDX5 and the accumulation of SUMOylated DDX5 (Supplementary Figures S3 and S4). Previously, we reported that Arf forces the accumulation of SUMOylated proteins in the nucleolus.[37] SUMOylation of DDX5 was reported to suppress the p53-mediated transcription by the interaction between SUMOylated DDX5 and HDAC1.[38] In the current study, we observed that Arf blocked the physical interaction between DDX5 and c-Myc, as shown in Figure 3c, and the SUMOylation of DDX5 induced by Arf might be the crucial step for the Arf-dependent inhibitory effect on c-Myc.

We also observed that short hairpin RNA-mediated knockdown of DDX5 caused p53-independent cell growth retardation, as with the induced expression of Arf (Supplementary Figure S5). This is well fitted with the result of soft agar colony formation assay as shown in Figures 5c and d. However, the reduction of cell growth of c-Myc-induced transformed cells by DDX5 knockdown did not show the drastic effect (Figure 5b). We do not have suitable

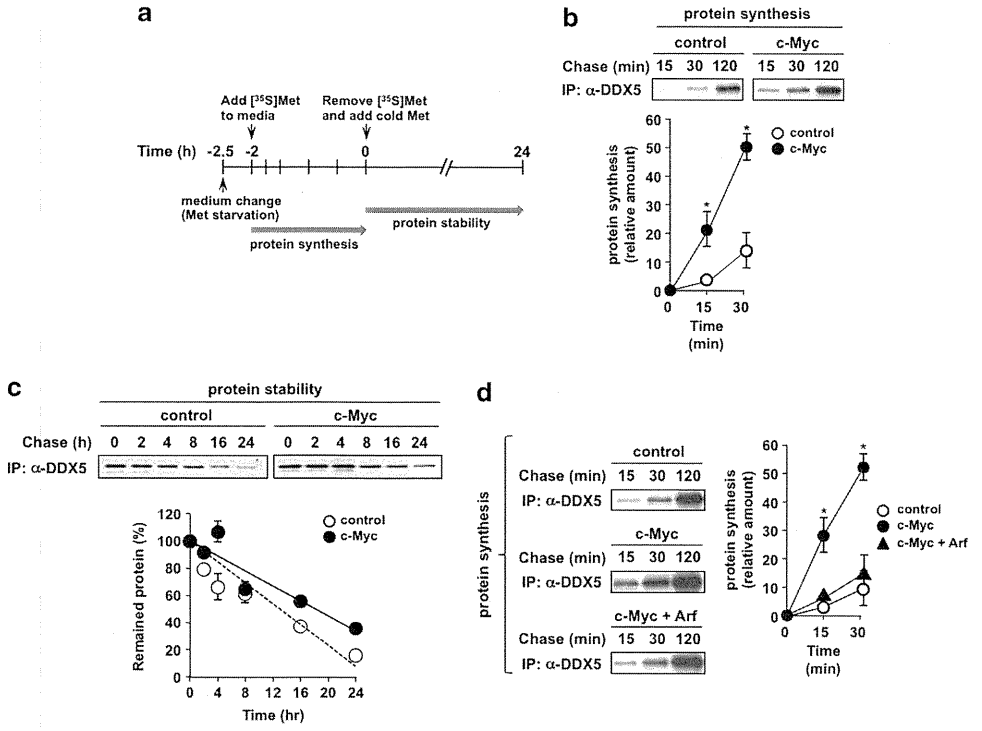

Figure 9. c-Myc accelerates the protein synthesis of DDX5. (**a**) Shows the time course of the experiments of **b** and **c**. TKO cells infected with control virus or retrovirus harboring c-Myc were labeled with [^{35}S] Met in the media as shown in figure. The effects of c-Myc on the protein synthesis and degradation of DDX5 in TKO cells are analyzed as shown in **b** and **c**, respectively. (**d**) Using TKO cells infected with the indicated combinations of retroviruses harboring c-Myc and/or Arf, the effect of Arf on the protein synthesis of DDX5 accelerated by c-Myc was evaluated. In the graph, error bars mean s.d. ($n=3$, $^*P<0.01$).

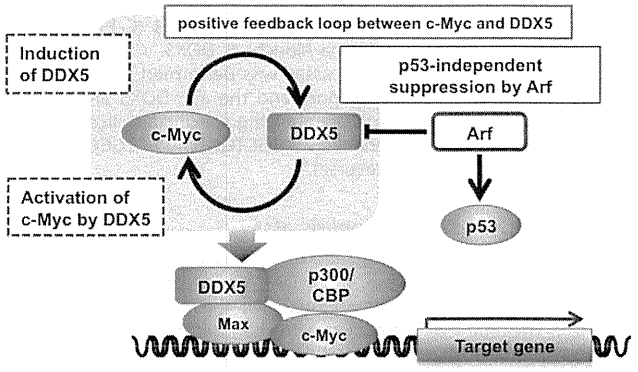

Figure 10. The working hypothesis in this study. c-Myc stabilizes DDX5 protein and DDX5 enhances the transcriptional activity of c-Myc (positive feedback loop). Arf blocks this interaction and suppresses the c-Myc-induced cellular transformation in a p53- and Mdm2-independent manner.

explanation for these differences; however, DDX5 may contribute to the anchorage-independent growth mediated by cancelling the anoikis. Additionally, the enforced expression of DDX5 alone failed to cause the cellular transformation (KT, unpublished data), suggesting that DDX5 does not harbor the sufficient role to substitute the function of c-Myc, although DDX5 is apparently the essential protein for the action of c-Myc. Previously, DDX5 was reported as a transcriptional coactivator of p53 activated by γ-irradiation; however, our current observation does not support this previous finding.[39] We showed that Arf-induced activation of p53 does not require DDX5 (Supplementary Figure S6). DNA damage-induced p53 activation is mediated by a p53-regulating protein kinase, ATM or ATR, but not Arf.[40] This discrepancy for DDX5 in the p53 activation may be caused by the difference of the p53 activator.

It is still unclear how DDX5 contributes to the activities of c-Myc, although DDX5 is clarified to be essential for c-Myc-induced expression of its target genes and cellular transformation. As shown in Supplementary Figure S1, DDX5 did not show the binding ability to TIP49, which is important for the action of c-Myc. Additionally, we also could not observe the interaction between DDX5 and a partner protein of c-Myc, Max (KT, unpublished data). These observations suggest that DDX5 is unlikely to contribute to the transcriptional activation of c-Myc. We observed that the activated Myc-ER prolonged the half-life of Odc mRNA in the cells treated with α-amanitin, an inhibitor of RNA polymerase II (KT, unpublished data), suggesting that c-Myc also stabilizes its transcripts. Thus far, without further supportive evidences, DDX5 may contribute to the mRNA stabilization of the target genes of c-Myc.

In the current study, we point out the presence of a positive feedback loop between c-Myc and DDX5. c-Myc enhanced the amount of DDX5 protein through acceleration of the protein synthesis of DDX5, but not the transcription of DDX5 mRNA (Figure 8a). However, we also observed that DNA-binding activity of c-Myc is required for the induction of DDX5 expression (Figure 8b), which suggests that c-Myc promotes the protein synthesis of DDX5 through the expression of c-Myc target genes, at least in part. Myc oncogenes such as c-Myc and N-Myc are reported to regulate multiple aspects of tumor metabolism including glycolysis and glutaminolysis.[41] In particular, c-Myc is broadly deregulated in many human tumors. Oncogenic c-Myc increases the glutaminolysis by cooperative activation of transcriptional and post-translational machinery.[42,43] c-Myc may utilize these metabolic disorders in tumor cells to accelerate the protein synthesis of DDX5. It has been well understood that mTORC1 contributes to the protein synthesis.[44] Recently, it was

reported that mTORC1 is activated by glutaminolysis; however, we could not observe the reduction of DDX5 expression by the treatment with rapamycin (KT, unpublished data).[45] It will be important to clarify the detailed mechanism by which c-Myc and DDX5 cause the oncogenic positive feedback loop, and how Arf disrupts it. In addition, analysis of other functions of DDX5, and the relationship between Arf and other members of DDX RNA helicases will also be interesting to consider the functions of Arf tumor suppressor. These studies would provide a clue to understand not only the p53-independent function of Arf tumor suppressor, but also the physiological functions including non-tumor suppressor roles of Arf protein comprehensively.

MATERIALS AND METHODS

Cells and culture conditions

NIH-3T3 fibroblasts were maintained in Dulbecco's modified Eagle's medium supplemented with 10% fetal calf serum, 2 mM glutamine and 100 units each of penicillin and streptomycin. MEFs from a C57BL/6 × 129 strain lacking the *Arf, p53* and *Mdm2* genes, called TKO cells, were cultured in complete medium supplemented with 0.1 mM nonessential amino acids, 55 μM 2-mercaptoethanol and 10 μg/ml of gentamycin instead of penicillin and streptomycin.[13,46]

Retrovirus production and infection

Human kidney 293T cells (HEK293T) were transfected as described with helper retrovirus plasmid together with murine stem cell virus (MSCV)–internal ribosome entry site (IRES)–green fluorescent protein (GFP) vectors encoding $p19^{ARF}$ proteins tagged with FLAG on the C terminus or with MSCV–IRES–GFP vector encoding tandem affinity purification-tagged Arf or MSCV–IRES–Puro vectors containing FLAG-tagged wild-type or mutant murine DDX5 proteins. Viruses were collected 24–60 h post-transfection, pooled, and stored on ice. Exponentially growing cells (2×10^5 cells per 10-cm-diameter culture dish) were infected twice at 2 h intervals with 2 ml of fresh virus-containing supernatant in complete medium containing 8 μg/ml polybrene (Sigma-Aldrich, St Louis, MO, USA). Infection efficiencies were confirmed by flow cytometric analysis of GFP-stained cells or puromycin selection.

Tandem affinity purification of tagged Arf protein

The cDNA fragment of Arf lacking a stop codon was amplified by PCR and inserted as an *Eco*RI/*Xho*I fragment into the cloning site of the cassette retroviral vector, MSCV–IRES–GFP harboring His_6-FLAG tandem tags. Cells infected with retrovirus encoding tandem affinity purification-tagged Arf proteins were collected and resuspended with 5 ml of hypotonic buffer (50 mM HEPES (pH 7.5), 10 mM KCl, 1 mM EDTA, 2.5 mM EGTA, 0.1% NP-40, 0.2 U/ml of aprotinin, 10 mM β-glycerophosphate, 1 mM NaF and 0.1 mM $NaVO_4$), and then nuclei were isolated by centrifugation (1000 × *g* for 5 min at 4 °C). Isolated nuclei were resuspended with 2 ml of Tween-20 lysis buffer (50 mM HEPES (pH 7.5), 150 mM NaCl, 1 mM EDTA, 2.5 mM EGTA, 0.1% Tween-20, 0.2 U/ml of aprotinin, 10 mM β-glycerophosphate, 1 mM NaF and 0.1 mM $NaVO_4$), and then sonicated briefly. Lysates were centrifuged at 14 000 × *g* at 4 °C for 15 min, and the resulting supernatants were loaded into M2 agarose (Sigma-Aldrich) and rotated for 90 min at 4 °C. The resin was washed four times with Tween-20 lysis buffer, and bound proteins were eluted twice with 200 μg/ml FLAG peptide in Tween-20 lysis buffer without EDTA and EGTA. Eluted fractions were next loaded into Ni-NTA agarose (Qiagen, Valencia, CA, USA) and rotated for 30 min at 4 °C. The resin was washed four times with Tween-20 lysis buffer (minus EDTA and EGTA), and then the protein complexes containing Arf were eluted with 300 mM imidazole in Tween-20 lysis buffer. The Arf-containing complexes were analyzed by MudPIT analysis.[47]

Construction of the expression plasmids for DDX5 and its mutants

Full-length murine DDX5 cDNA was cloned from total RNA of NIH-3T3 cells by reverse transcription–PCR with its specific primers (sense primer: 5′-TTTGAATTCATGTCGAGTTATTCTAG-3′ (primer-p68F); antisense primer: 5′-TTTCTCGAGTTATTGAGAATACCCTG-3′ (primer-p68R)). Deletion mutants were generated by PCR as follows: N134 mutant was amplified with sense primer (5′-AAAGAATTCATGGTTGGAGTAGCTCAG-3′) and primer-p68R; C430 was amplified by PCR with primer-p68F and antisense primer (5′-TTTCTCGAGTCATCCAATTCGATGAATATAATC-3′); C554 was amplified with primer-p68F and antisense primer (5′-TTTCTCGAGTCATATGCCAGCA GATAC-3′). ΔCat mutant was produced using the quikchange mutagenesis kit (Agilent Technologies, Santa Clara, CA, USA). pcDNA3-FLAG-p68 DDX5 (full length) was used as a template, and primers were as follows: sense: 5′-GTTGCTCTCAGTGGATTGGATATGAGAACTGCTCGCAGTACCAAAA-3′; antisense: 5′-TTTTGGTACTGCGAGCAGTTCTCATATCCAATCCACTGAGAGCAAC-3′. PCR products were digested with *Eco*RI and *Xho*I, purified and cloned into pcDNA3 or MSCV–IRES–GFP vectors containing N-terminal FLAG tag-coding sequences.

RNA interference for DDX5

Annealed oligonucleotide coding short hairpin RNA for murine DDX5 was inserted into pSUPER-retro-puro retroviral plasmid (Oligoengine, Seattle, WA, USA). The sequences of oligonucleotides used for constructing the short hairpin RNA retroviral vector were as follows: 5′-GATCCCCGTAGATAC ATACAGAAGAATTCAAGAGATTCTTCTGTATGTATCTACTTTTTA-3′ and 5′-AGC TTAAAAAGTAGATACATACAGAAGAATCTCTTGAATTCTTCTGTATGTATCTACG GG-3′ (underlined sequences correspond to the sequence of murine DDX5, from 217 to 235 in ORF).

Immunoprecipitation, immunoblotting and chromatin immunoprecipitation assay

Cells were suspended in RIPA buffer (10 mM Na phosphate (pH 7.2), 150 mM NaCl, 2 mM EDTA, 1% NP-40, 1% sodium deoxycholate, 0.2 U/ml aprotinin and phosphatase inhibitors) or Tween-20 buffer and briefly sonicated on ice. Lysates cleared by sedimentation in a microcentrifuge at 14 000 r.p.m. for 10 min were precipitated for 2 h at 4 °C with indicated antibodies (anti-DDX5 antibody (Merck Millipore, Billerica, MA, USA), anti-FLAG antibody (M2) (Sigma-Aldrich) or antibody to $p19^{ARF}$ antibody (5C3, Santa Cruz Biotechnology, Santa Cruz, CA, USA)). Immune complexes were recovered with protein G- or protein A-Sepharose (GE Healthcare Biosciences, Pittsburgh, PA, USA) and washed four times with RIPA buffer or Tween-20 buffer. Immunoprecipitated complexes and total cell lysates were electrophoretically separated on denaturing polyacrylamide gels and transferred to polyvinylidene difluoride membranes (Merck Millipore). Proteins were detected with antibodies to Arf, p53 (Ab-7, Oncogene Research Products, San Diego, CA, USA), p21Cip1 (C-19, Santa Cruz Biotechnology), NPM (C-19, Santa Cruz Biotechnology), FLAG tag (M2, Sigma-Aldrich) or DDX5.

Chromatin immunoprecipitation assay was performed on infected TKO MEFs using a kit from Merck Millipore and the anti-DDX5 antibody. The sequences of primers used for PCR amplifying specific amplicon including E-box sequences in the *Odc* gene were AGGCTGGTGACCTTGCGA (forward) and TGACACGATGCGGGCTC (reverse).[48]

Soft agar assay and tumorigenesis assay

TKO cells infected with the indicated retroviruses were seeded onto soft agar at 10^4 cells per 35-mm dish, and grown for 3 weeks. After 3 weeks, the number of visible colonies was counted. For the tumorigenesis assay in nude mice, TKO MEFs were infected with the indicated retroviruses. MEFs were trypsinized and resuspended in phosphate-buffered saline at a concentration of 2×10^7 cells/ml. Nude mice were injected subcutaneously with 2×10^6 cells, with sample sizes of five mice per condition. Tumor size was measured during 21 days after the inoculation of transformed cells using calipers to measure the tumors in two dimensions. Tumor volume was calculated as described previously.[33]

Quantitative reverse transcription–PCR

NIH-3T3 cells or TKO MEFs infected with control retrovirus (pBabePuro) or virus harboring Myc-ER were treated with/without 4-HT for 3 h. Total RNA was extracted and used for quantitative PCR using primers for Myc target gene, *Odc* and internal control gene, *ubiquitin*, as well as *DDX5*. The expressions of *Odc* and *DDX5* were normalized using the expression of *ubiquitin*, and shown in the graphs.

Metabolic labeling experiment

TKO MEFs infected with the indicated combination of retroviruses were cultured in Dulbecco's modified Eagle's medium without methionine and cysteine for 30 min. Then, [^{35}S] methionine and cysteine (Perkin-Elmer, Waltham, MA, USA) were added to the culture. Cells were collected at the indicated time points (15, 30, 120 min), and utilized for immunoprecipitation assay. Then, proteins were resolved by SDS–polyacrylamide

gelelectrophoresis, and intensities of each band were measured. After 120 min of incubation, the incorporation of ^{35}S into the precipitated DDX5 reached a plateau in each sample, and we calculated the relative amount of ^{35}S incorporation in DDX5. In the case of protein stability, after labeling with [^{35}S] methionine and cysteine for 2 h, cells started to be cultured in complete medium including an excess amount of cold methionine and cysteine. Cells were collected at the indicated time points and utilized for immunoprecipitation assay.

CONFLICT OF INTEREST

The authors declare no conflict of interest.

ACKNOWLEDGEMENTS

We thank Charles Sherr and Martine Roussel for critical advice and reagents, and Michael Washburn of Stowers Institute for Medical Research Proteomics Center for performing MudPIT analysis. This work was supported by a grant-in-aid for scientific research from the MEXT (20770103), MEXT-supported program for the strategic research foundation at private universities (2013–2017) and the Takeda Science Foundation.

REFERENCES

1 Serrano M, Hannon GJ, Beach D. A new regulatory motif in cell-cycle control causing specific inhibition of cyclin D/CDK4. *Nature* 1993; **366**: 704–707.
2 Quelle DE, Zindy F, Ashmun RA, Sherr CJ. Alternative reading frames of the INK4a tumor suppressor gene encode two unrelated proteins capable of inducing cell cycle arrest. *Cell* 1995; **83**: 993–1000.
3 Kamijo T, Zindy F, Roussel MF, Quelle DE, Downing JR, Ashmun RA *et al.* Tumor suppression at the mouse INK4a locus mediated by the alternative reading frame product p19ARF. *Cell* 1997; **91**: 649–659.
4 Zhang Y, Xiong Y, Yarbrough WG. ARF promotes MDM2 degradation and stabilizes p53: ARF-INK4a locus deletion impairs both the Rb and p53 tumor suppression pathways. *Cell* 1998; **92**: 725–734.
5 Kamijo T, Weber JD, Zambetti G, Zindy F, Roussel MF, Sherr CJ. Functional and physical interactions of the ARF tumor suppressor with p53 and Mdm2. *Proc Natl Acad Sci USA* 1998; **95**: 8292–8297.
6 Honda R, Yasuda H. Association of $p19^{ARF}$ with Mdm2 inhibits ubiquitin ligase activity of Mdm2 for tumor suppressor p53. *EMBO J* 1999; **18**: 22–27.
7 Dornan D, Wertz I, Shimizu H, Arnott D, Frantz GD, Dowd P *et al.* The ubiquitin ligase COP1 is a critical negative regulator of p53. *Nature* 2004; **429**: 86–92.
8 Chen D, Kon N, Li M, Zhang W, Qin J, Gu W. ARF-BP1/Mule is a critical mediator of the ARF tumor suppressor. *Cell* 2005; **121**: 1071–1083.
9 Kelly-Spratt KS, Gurley KE, Yasui Y, Kemp CJ. $p19^{Arf}$ suppresses growth, progression, and metastasis of H-ras-driven carcinomas through p53-dependent and-independent pathways. *PLoS Biol* 2004; **2**: 1138–1149.
10 Carnero A, Hudson JD, Price CM, Beach DH. $p16^{INK4A}$ and $p19^{ARF}$ act in overlapping pathways in cellular immortalization. *Nat Cell Biol* 2000; **2**: 148–155.
11 Eischen CM, Weber JD, Roussel MF, Sherr C, Cleveland JL. Disruption of the ARF-Mdm2-p53 tumor suppressor pathway in Myc-induced lymphomagenesis. *Genes Dev* 1999; **13**: 2658–2669.
12 Weber JD, Jeffers JR, Rehg JE, Randle DH, Lozano G, Roussel MF *et al.* p53-independent functions of the $p19^{ARF}$ tumor suppressor. *Genes Dev* 2000; **14**: 2358–2365.
13 Sugimoto M, Kuo ML, Roussel MF, Sherr CJ. Nucleolar Arf tumor suppressor inhibits ribosomal RNA processing. *Mol Cell* 2003; **11**: 415–424.
14 Itahana K, Bhat KP, Jin A, Itahana Y, Hawke D, Kobayashi R *et al.* Tumor suppressor ARF degrades B23, a nucleolar protein involved in ribosome biogenesis and cell proliferation. *Mol Cell* 2003; **12**: 1151–1164.
15 Bertwistle D, Sugimoto M, Sherr CJ. Physical and functional interactions of the Arf tumor suppressor protein with nucleophosmin/B23. *Mol Cell Biol* 2004; **24**: 985–996.
16 Martelli F, Hamilton T, Silver DP, Sharpless NE, Bardeesy N, Rokas M *et al.* $p19^{ARF}$ targets certain E2F species for degradation. *Proc Natl Acad Sci USA* 2001; **98**: 4455–4460.
17 Eymin B, Karayan L, Seite P, Brambilla C, Brambilla E, Larsen CJ *et al.* Human ARF binds E2F1 and inhibits its transcriptional activity. *Oncogene* 2001; **20**: 1033–1041.
18 Datta A, Nag A, Pan W, Hay N, Gartel AL, Colamonici O *et al.* Myc-ARF (alternate reading frame) interaction inhibits the functions of Myc. *J Biol Chem* 2004; **279**: 36698–36707.
19 Qi Y, Gregory MA, Li Z, Brousal JP, West K, Hann SR. $p19^{ARF}$ directly and differentially controls the functions of c-Myc independently of p53. *Nature* 2004; **431**: 712–717.
20 Rocha S, Campbell KJ, Perkins ND. p53- and Mdm2-independent repression of NF-κB transactivation by the ARF tumor suppressor. *Mol Cell* 2003; **12**: 15–25.
21 Xirodimas DP, Chisholm J, Desterro JM, Lane DP, Hay RT. $p14^{ARF}$ promotes accumulation of SUMO-1 conjugated (H) Mdm2. *FEBS Lett* 2002; **528**: 207–211.
22 Chen L, Chen J. MDM2-ARF complex regulates p53 sumoylation. *Oncogene* 2003; **22**: 5348–5357.
23 Kuo ML, den Besten W, Thomas MC, Sherr CJ. Arf-induced turnover of the nucleolar nucleophosmin-associated SUMO-2/3 protease Senp3. *Cell Cycle* 2008; **7**: 3378–3387.
24 Lane DP, Hoeffler WK. SV40 large T shares an antigenic determinant with a cellular protein of molecular weight 68 000. *Nature* 1980; **288**: 167–170.
25 Hirling H, Scheffner M, Restle T, Stahl H. RNA helicase activity associated with the human p68 protein. *Nature* 1989; **339**: 562–564.
26 Heinlein UA. Dead box for the living. *J Pathol* 1998; **184**: 345–347.
27 Stevenson RJ, Hamilton SJ, MacCallum DE, Hall PA, Fuller-Pace FV. Expression of the 'dead box' RNA helicase p68 is developmentally and growth regulated and correlates with organ differentiation/maturation in the fetus. *J Pathol* 1998; **184**: 351–359.
28 Dubey P, Hendrickson RC, Meredith SC, Siegel CT, Shabanowitz J, Skipper JC *et al.* The immunodominant antigen of an ultraviolet-induced regressor tumor is generated by a somatic point mutation in the DEAD box helicase p68. *J Exp Med* 1997; **185**: 695–705.
29 Causevic M, Hislop RG, Kernohan NM, Carey FA, Kay RA, Steele RJ *et al.* Overexpression and poly-ubiquitylation of the DEAD-box RNA helicase p68 in colorectal tumours. *Oncogene* 2001; **20**: 7734–7743.
30 Yang L, Lin C, Liu ZR. Phosphorylations of DEAD box p68 RNA helicase are associated with cancer development and cell proliferation. *Mol Cancer Res* 2005; **3**: 355–363.
31 Yang L, Lin C, Liu ZR. P68 RNA helicase mediates PDGF-induced epithelial mesenchymal transition by displacing Axin from beta-catenin. *Cell* 2006; **127**: 139–155.
32 Saporita AJ, Chang HC, Winkeler CL, Apicelli AJ, Kladney RD, Wang J *et al.* RNA Helicase DDX5 Is a p53-Independent Target of ARF That Participates in Ribosome Biogenesis. *Cancer Res* 2011; **71**: 6708–6717.
33 Eilers M, Schirm S, Bishop JM. The MYC protein activates transcription of the α-prothymosin gene. *EMBO J* 1991; **10**: 133–141.
34 Littlewood TD, Hancock DC, Danielian PS, Parker MG, Evan GI. A modified oestrogen receptor ligand-binding domain as an improved switch for the regulation of heterologous proteins. *Nucleic Acids Res* 1995; **23**: 1686–1690.
35 Packham G, Cleveland JL. Induction of ornithine decarboxylase by IL-3 is mediated by sequential c-Myc-independent and c-Myc-dependent pathways. *Oncogene* 1997; **15**: 1219–1232.
36 Chang DW, Claassen GF, Hann SR, Cole MD. The c-Myc transactivation domain is a direct modulator of apoptotic versus proliferative signals. *Mol Cell Biol* 2000; **20**: 4309–4319.
37 Tago K, Chiocca S, Sherr CJ. Sumoylation induced by the Arf tumor suppressor: a p53-independent function. *Proc Natl Acad Sci USA* 2005; **102**: 7689–7694.
38 Jacobs AM, Nicol SM, Hislop RG, Jaffray EG, Hay RT, Fuller-Pace FV. SUMO modification of the DEAD box protein p68 modulates its transcriptional activity and promotes its interaction with HDAC1. *Oncogene* 2007; **26**: 5866–5876.
39 Bates GJ, Nicol SM, Wilson BJ, Jacobs AM, Bourdon JC, Wardrop J *et al.* The DEAD box protein p68: a novel transcriptional coactivator of the p53 tumour suppressor. *EMBO J* 2005; **24**: 543–553.
40 Reinhardt HC, Yaffe MB. Kinases that control the cell cycle in response to DNA damage: Chk1, Chk2, and MK2. *Curr Opin Cell Biol* 2009; **21**: 245–255.
41 Dang CV. MYC on the path to cancer. *Cell* 2012; **149**: 22–35.
42 Gao P, Tchernyshyov I, Chang TC, Lee YS, Kita K, Ochi T *et al.* c-Myc suppression of miR-23a/b enhances mitochondrial glutaminase expression and glutamine metabolism. *Nature* 2009; **458**: 762–765.
43 Wise DR, DeBerardinis RJ, Mancuso A, Sayed N, Zhang XY, Pfeiffer HK *et al.* Myc regulates a transcriptional program that stimulates mitochondrial glutaminolysis and leads to glutamine addiction. *Proc Natl Acad Sci USA* 2008; **105**: 18782–18787.
44 Martin DE, Powers T, Hall MN. Regulation of ribosome biogenesis: where is TOR? *Cell Metab* 2006; **4**: 259–260.
45 Durán RV, Oppliger W, Robitaille AM, Heiserich L, Skendaj R, Gottlieb E *et al.* Glutaminolysis activates Rag-mTORC1 signaling. *Mol Cell* 2012; **47**: 349–358.
46 Zindy F, Eischen CM, Randle DH, Kamijo T, Cleveland JL, Sherr CJ *et al.* Myc signaling via the ARF tumor suppressor regulates p53-dependent apoptosis and immortalization. *Genes Dev* 1998; **12**: 2424–2433.
47 Washburn MP, Wolters D, Yates 3rd JR. Large-scale analysis of the yeast proteome by multidimensional protein identification technology. *Nat Biotechnol* 2001; **19**: 242–247.
48 Frank SR, Schroeder M, Fernandez P, Taubert S, Amati B. Binding of c-Myc to chromatin mediates mitogen-induced acetylation of histone H4 and gene activation. *Genes Dev* 2001; **15**: 2069–2082.

Supplementary Information accompanies this paper on the Oncogene website (http://www.nature.com/onc)

Oncogene (2013) **32,** 1670–1681

www.nature.com/onc

ORIGINAL ARTICLE

BCR-ABL regulates death receptor expression for TNF-related apoptosis-inducing ligand (TRAIL) in Philadelphia chromosome-positive leukemia

I Kuroda[1], T Inukai[1], X Zhang[1,6], J Kikuchi[2], Y Furukawa[2], A Nemoto[1], K Akahane[1], K Hirose[1], H Honna-Oshiro[1], K Goi[1], K Kagami[1], H Yagita[3], T Tauchi[4], Y Maeda[5] and K Sugita[1]

Allogeneic stem cell transplantation (allo-SCT) is a potentially curative therapy for chronic myeloid leukemia and Philadelphia chromosome-positive (Ph(+)) acute lymphoblastic leukemia, and the graft-vs-leukemia (GVL) effect can eradicate residual leukemia after allo-SCT. Ph(+) leukemia cells frequently express death-inducing receptors (DR4 and DR5) for tumor necrosis factor-related apoptosis-inducing ligand (TRAIL), which is one of the cytotoxic ligands expressed on cytotoxic T cells and natural killer cells mediating the GVL effect. Here we demonstrate that imatinib specifically downregulated DR4 and DR5 expression in cell lines and clinical samples of Ph(+) leukemia. Second-generation tyrosine kinase inhibitors (dasatinib and nilotinib) and short hairpin RNA against *bcr-abl* also downregulated DR4 and DR5 expression in Ph(+) leukemia cells, and transfection of *bcr-abl* into a Ph(−) leukemia cell line induced DR4 and DR5 expression, which was abrogated by imatinib treatment. Accordingly, Ph(+) leukemia cells that had been pretreated with imatinib showed resistance to the pro-apoptotic activity of recombinant human soluble TRAIL. These observations demonstrate that BCR-ABL is critically involved in the leukemia-specific expression of DR4 and DR5 and in the susceptibility of Ph(+) leukemia to TRAIL-mediated anti-leukemic activity, providing new insight into the mechanisms of the tumor-specific cytotoxic activities of TRAIL.

Oncogene (2013) **32,** 1670–1681; doi:10.1038/onc.2012.186; published online 4 June 2012

Keywords: Philadelphia chromosome-positive leukemia; tumor necrosis factor-related apoptosis-inducing ligand; BCR-ABL

INTRODUCTION

Chronic myeloid leukemia (CML) is a clonal myeloproliferative disorder characterized by the Philadelphia chromosome (Ph), which results from a t(9;22) (q34;q11) chromosome translocation.[1–3] Approximately 20%[4] of adult and 5%[5] of childhood acute lymphoblastic leukemia (ALL) and 2%[2] of acute myeloblastic leukemia cases are also positive for Ph. The Ph carries the *bcr-abl* fusion gene, which encodes a chimeric protein termed BCR-ABL with upregulated tyrosine kinase activity,[1–3] that has a central role in the promotion of cell survival and proliferation of Ph(+) leukemia cells. Imatinib mesylate (Gleevec) (Druker *et al.*[6]), an inhibitor of the kinase activity of BCR-ABL, became the standard therapy for all stages of CML[7] as well as Ph(+) ALL[8] and more potent second-generation tyrosine kinase inhibitors (TKIs), dasatinib and nilotinib, have also recently been approved by the health authorities.[2,9,10] Allogeneic stem cell transplantation (allo-SCT) is another therapy for the chronic phase of CML, as well as blastic crisis of CML (CML-BC) and Ph(+) ALL,[2,11,12] and is potentially curative. The graft-vs-leukemia (GVL) effect has a critical role in achieving a cure in patients with CML and Ph(+) ALL after allo-SCT.[2] The GVL effect is mediated by cytotoxic T lymphocytes and natural killer cells,[13,14] and death receptor ligands including FasL and tumor necrosis factor-related apoptosis-inducing ligand (TRAIL) have an important role in cytotoxic T-lymphocyte- and natural killer cell-mediated anti-tumor immunity.[15–22] In bone marrow transplantation models using TRAIL-deficient mice, TRAIL was required for optimal graft-vs-tumor activity, whereas it played little or no role in the development of graft-vs-host disease.[21] TRAIL triggers apoptosis of tumor cells by binding to its death domain-containing receptors, DR4[23] (TRAIL-R1) and DR5[24] (TRAIL-R2). We previously showed that Ph(+) leukemia cells frequently express DR4 and/or DR5 and are sensitive to the anti-leukemic activity of recombinant human soluble (rhs) TRAIL in contrast to their relative resistance to rhs FasL due to limited expression of Fas.[25] Accordingly, DR4 and DR5 expression on Ph(+) leukemias could mediate the GVL effect after allo-SCT at least in part.

Despite the importance of DR4 and DR5 expression on tumor cells for anti-tumor immunity,[26] there are very limited findings regarding the mechanisms for the expression of DR4 and DR5 on tumor cells. Considering the frequent expression of DR4 and DR5 on Ph(+) leukemias and resultant susceptibility to the anti-leukemic activity of rhs TRAIL,[25] it is feasible to predict that BCR-ABL itself may be involved in expression of DR4 and DR5 in Ph(+) leukemia cells. Our recent analysis on the effect of imatinib on TRAIL-resistant Ph(+) leukemia cells supports this assumption.[27] Thus, in the present study, we attempted to clarify the possible involvement of BCR-ABL in the expression of DR4 and DR5. We

[1]Department of Pediatrics, School of Medicine, University of Yamanashi, Yamanashi, Japan; [2]Stem Cell Regulation, Center for Molecular Medicine, Jichi Medical School, Tochigi, Japan; [3]Department of Immunology, Juntendo University School of Medicine, Tokyo, Japan; [4]First Department of Internal Medicine, Tokyo Medical University, Tokyo, Japan and [5]Department of Internal Medicine, Division of Hematology, Kinki University School of Medicine, Osaka, Japan. Correspondence: Dr T Inukai, Department of Pediatrics, School of Medicine, University of Yamanashi, 1110 Shimokato, Chuo, Yamanashi 409-3898, Japan.
E-mail: tinukai@yamanashi.ac.jp
[6]Current address: Department of Pediatrics, The General Hospital of Ningxia Medical University, Ningxia, China
Received 12 September 2011; revised 7 March 2012; accepted 6 April 2012; published online 4 June 2012

found that imatinib and short hairpin RNA (shRNA) against *bcr-abl* downregulated gene and cell surface expression of DR4 and DR5 in Ph(+) leukemia cells, whereas transfection of *bcr-abl* into a Ph(−) leukemia cell line induced DR4 and DR5 expression. These observations demonstrate that BCR-ABL is critically involved in the Ph(+) leukemia-specific expression of DR4 and DR5.

RESULTS

TKIs downregulate DR4 and DR5 expression on Ph(+) leukemia cells

We analyzed the effect of imatinib on cell surface expression of DR4 and DR5 in KOPM30, an imatinib-sensitive Ph(+) acute myeloblastic leukemia cell line expressing DR4 and DR5 but not

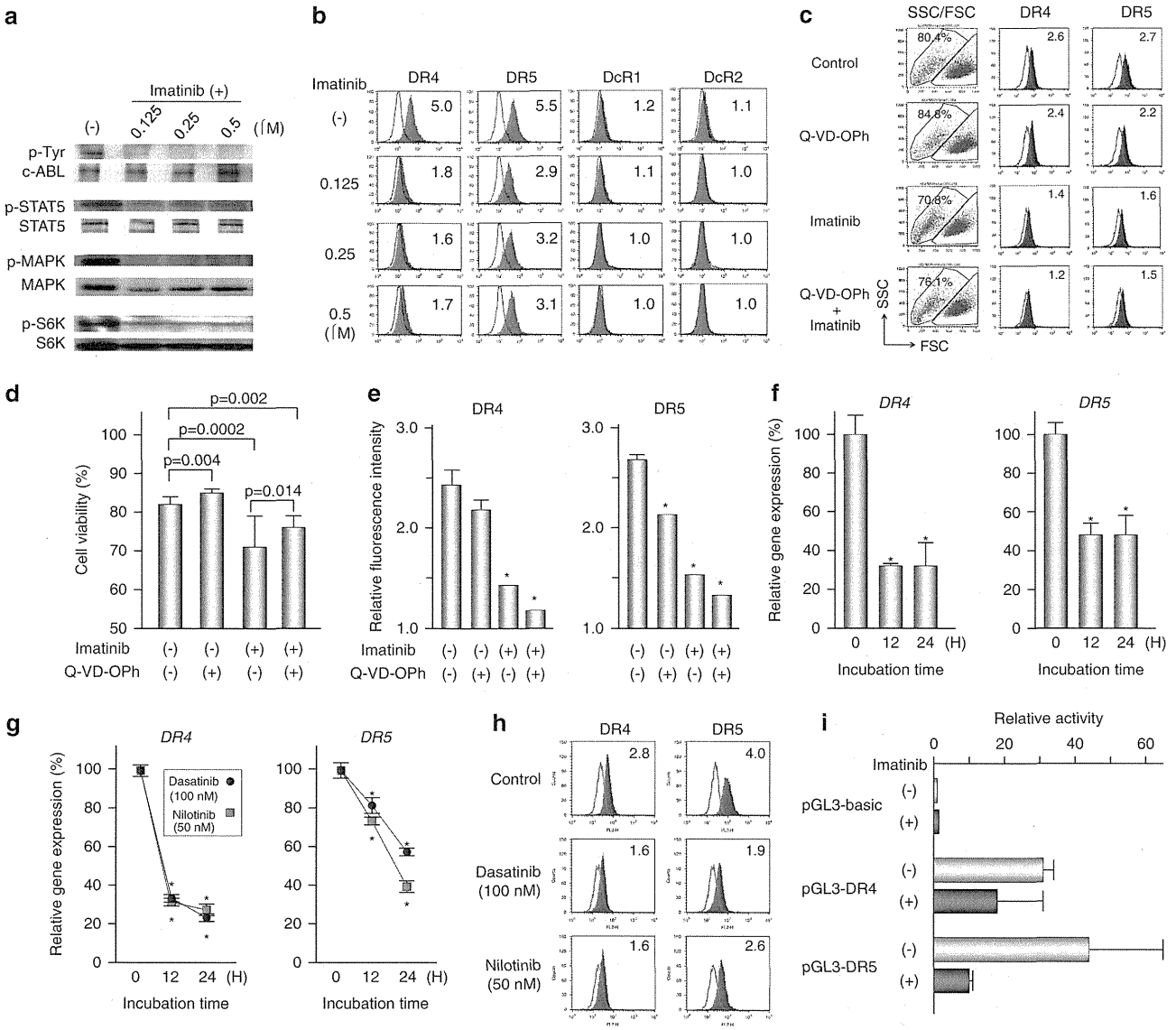

Figure 1. DR4 and DR5 expression in KOPM30 treated with TKIs. (**a**) Imatinib-induced dephosphorylation of BCR-ABL and downstream signaling molecules in KOPM30 cells. Cells were incubated with imatinib for 2 h and harvested for immunoblotting. (**b**) Cell surface expression of DR4, DR5, DcR1 and DcR2 in KOPM30 cells treated with imatinib. Cells cultured in the absence or presence of imatinib for 24 h were analyzed for DR4, DR5, DcR1 and DcR2 expression by flow cytometry. Relative fluorescence intensity (RFI) is indicated. (**c**–**e**) Viability and cell surface expression of DR4 and DR5 in imatinib-treated KOPM30 cells in the absence or presence of Q-VD-OPh. Cells cultured in the absence or presence of Q-VD-OPh (10 μM) with imatinib (0.5 μM) for 24 h were analyzed for the side scatter/forward scatter fraction and DR4 and DR5 expression by flow cytometry (**c**). Cell viability (**d**) and RFI of cell surface expression of DR4 and DR5 (**e**) are indicated with error bars (standard division) in triplicate experiments. (**f** and **g**) Gene expression of *DR4* and *DR5* in KOPM30 cells treated with TKIs. Cells cultured in the absence or presence of (**f**) imatinib (0.5 μM), (**g**) dasatinib (100 nM) or nilotinib (50 nM) for 12 and 24 h were analyzed for *DR4* and *DR5* gene expression by real-time reverse transcriptase PCR (RT–PCR) using *GAPDH* as an internal control. Relative gene expression levels are indicated with error bars in triplicate experiments. Asterisk indicates a significant difference ($P<0.01$, *t*-test) compared with time 0. (**h**) Cell surface expression of DR4 and DR5 in KOPM30 cells treated with dasatinib and nilotinib. Cells cultured in the absence or presence of dasatinib (100 nM) or nilotinib (50 nM) for 24 h were analyzed for DR4 and DR5 expression by flow cytometry. RFI is indicated. (**i**) Luciferase assay for promoter activities of the *DR4* and *DR5* genes in KOPM30 cells. Cells were transiently transfected with pGL3-basic, pGL3-DR4 or pGL3-DR5 reporter plasmids, and subsequently, 24 h after transfection, cultured in the absence or presence of imatinib (0.2 μM) for 24 h. Luciferase assay was performed using a cotransfected *Renilla* luciferase construct as a control for normalization of transfection efficiencies, and relative luciferase activity against pGL3-basic vector is indicated with error bars in triplicate experiments.

the decoy receptors DcR1 and DcR2.[24,28] Imatinib efficiently dephosphorylated tyrosine residues of BCR-ABL and also dephosphorylated downstream signaling molecules of BCR-ABL such as signal transducer and activator of transcription (STAT)5, mitogen-activated protein kinase (MAPK) and p70S6K at a concentration of as low as 0.125 μM (Figure 1a). Of note, imatinib downregulated cell surface expression of DR4 and DR5 at a concentration of as low as 0.125 μM, but showed no effect on the DcR1 and DcR2 expression (Figure 1b). To rule out the possibility that imatinib-induced cell death somehow downregulated DR4 and DR5 expression, we next monitored DR4 and DR5 expression on imatinib-treated KOPM30 cells in the presence or absence of Q-VD-OPh, a pan-caspase inhibitor. After 48 h incubation with imatinib, when assessed by side scatter/forward scatter, cell viability of KOPM30 was moderately decreased from 81 to 72% in the absence of Q-VD-OPh, and it was partially recovered to 76% in the presence of Q-VD-OPh (Figures 1c and d). Although Q-VD-OPh itself weakly downregulated DR4 and DR5, imatinib-induced downregulation of DR4 and DR5 was not recovered in the presence of Q-VD-OPh (Figures 1c and e), suggesting that induction of cell death was not the mechanism of DR4/DR5 downregulation by imatinib treatment. Consistent with the cell surface expression, imatinib downregulated gene expression of *DR4* and *DR5* (Figure 1c). Not only imatinib but also dasatinib and nilotinib similarly downregulated gene (Figure 1d) and cell surface (Figure 1e) expression of DR4 and DR5. Finally, the luciferase assay demonstrated that imatinib downregulated *DR4* and *DR5* gene promoter activities (Figure 1f).

We next analyzed the effect of imatinib on DR4 and DR5 expression on both Ph(+) (KOPN66bi and YAMN91) and Ph(−)

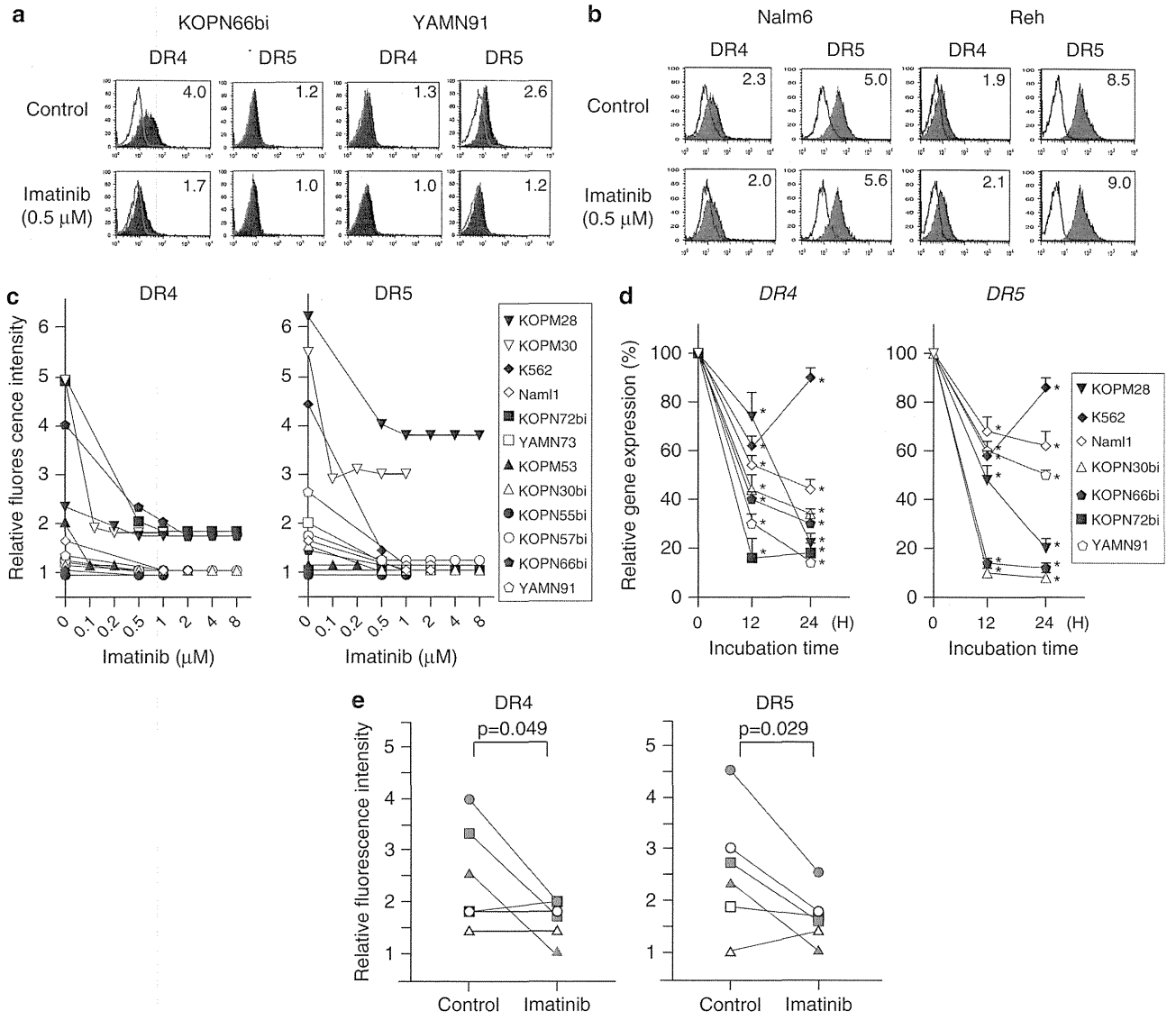

Figure 2. Specific downregulation of DR4 and DR5 expression in Ph(+) leukemia by imatinib. (**a** and **b**) Cell surface expression of DR4 and DR5 in (**a**) Ph(+) leukemia cell lines KOPN66bi and YAMN91 and (**b**) Ph(−) leukemia cell lines Nalm6 and Reh treated with imatinib. Cells cultured in the absence or presence of imatinib at 0.5 μM for 24 h were analyzed for DR4 and DR5 expression by flow cytometry. RFI is indicated. (**c**) Changes in RFI for DR4 and DR5 of 12 Ph(+) leukemia cell lines cultured in the absence or presence of imatinib. The vertical axis indicates RFI and the horizontal axis indicates the concentration of imatinib. (**d**) Changes in gene expression level of *DR4* and *DR5* in Ph(+) leukemia cell lines cultured in the presence of 0.5 μM imatinib for 12 and 24 h. Gene expression levels of *DR4* and *DR5* were quantified by real-time RT–PCR using *GAPDH* as an internal control. Relative gene expression levels are indicated with error bars in triplicate experiments. Asterisk indicates significant difference ($P<0.01$, *t*-test) compared with time 0. (**e**) Changes in RFI for DR4 and DR5 of clinical samples from six Ph(+) ALL patients cultured in the absence or presence of 0.5 μM imatinib for 24 h. *P*-values in paired *t*-test are indicated.

(Nalm6 and Reh) B-precursor ALL cell lines that expressed DR4 and/or DR5 at considerable levels. Imatinib (0.5 μM) efficiently downregulated DR4 and DR5 expression on KOPN66bi and YAMN91 (Figure 2a), whereas it did not downregulate DR4 and DR5 expression on Nalm6 and Reh (Figure 2b). We analyzed a total of 12 Ph(+) leukemia cell lines and confirmed that imatinib downregulated cell surface expression of DR4 and DR5 in all cell lines (Figure 2c). Moreover, downregulation of gene expression of *DR4* and *DR5* by imatinib was documented in all seven Ph(+) leukemia cell lines tested (Figure 2d). Finally, we analyzed the effect of imatinib on DR4 and DR5 expression in clinical samples from six Ph(+) ALL patients. Imatinib (0.5 μM) significantly downregulated cell surface expression of DR4 and DR5 in three and four out of six samples, respectively, and, as a whole, there was a statistically significant reduction in both DR4 and DR5 expression levels (Figure 2e).

Inactivation of BCR-ABL specifically downregulates DR4 and DR5 expression on Ph(+) leukemia cells

To verify the specificity of imatinib-induced DR4 and DR5 downregulation in Ph(+) leukemia cells, we tested an imatinib-resistant Ph(+) leukemia cell line that carries a T315I mutation. SU-Ph2 is an imatinib-sensitive Ph(+) ALL cell line that expresses DR4 and DR5 and is sensitive to rhs TRAIL, whereas SU/SR is its imatinib-resistant subline having the T315I mutation (Figure 3a).[29] Imatinib effectively dephosphorylated BCR-ABL (Figure 3a) and downregulated gene (Figure 3b) and cell surface expression (Figure 3c) of DR4 and DR5 in SU-Ph2, but much less so in SU/SR cells.

To further verify that inactivation of BCR-ABL downregulates DR4 and DR5 expression, we analyzed the effect of shRNA against *bcr-abl*. Using a lentivirus vector that contains green fluorescent protein (GFP) cDNA for cell sorting, we infected two sets of shRNA-expressing vector for *bcr-abl* (shRNA no. 1 and 3), as well as control vector containing ineffective oligonucleotides into KOPM30 cells. Protein expression of BCR-ABL was markedly downregulated both in the shRNA no. 1 virus-infected KOPM30 (shRNA no. 1/KOPM30) cells and in the shRNA no. 3 virus-infected KOPM30 (shRNA no. 3/KOPM30) cells compared with the control virus-infected KOPM30 (control/KOPM30) cells 24 h after infection (Figure 3d). Time course analysis of the GFP-positive population demonstrated that the percentage of the GFP-positive population was markedly lower in shRNA no. 1/KOPM30 and shRNA no. 3/KOPM30 cells compared with control/KOPM30 cells (Figure 3e) 36 h after infection, suggesting that gene inactivation of *bcr-abl* strongly induces cell death and/or cell cycle arrest of KOPM30 cells. The gene expression of *bcr-abl* in the GFP-positive population of shRNA/KOPM30 cells was 57 (shRNA no. 1) and 41% (shRNA no. 3) of that in control/KOPM30 cells (Figure 3f) 48 h after infection. Of note, gene (Figure 3g) and cell surface expression (Figure 3h) of DR4 and DR5 were significantly downregulated in shRNA/KOPM30 cells in comparison with control/KOPM30 cells 48 h after infection. Downregulation of cell surface expression of DR4 and DR5 in shRNA no. 3/KOPM30 cells was similarly observed in the presence of Q-VD-OPh (Figure 3h).

Introduction of BCR-ABL induces DR4/DR5 expression

As the above observations demonstrate that inactivation of BCR-ABL downregulates DR4 and DR5 expression in Ph(+) leukemia cells, we next tested if transfection of *bcr-abl* into Ph(−) leukemia cells upregulates DR4 and DR5 expression using a BCR-ABL-transfected granulocyte/macrophage-colony stimulating factor-dependent TF1 cell line (Figure 4a). In the presence of granulocyte/macrophage-colony stimulating factor, gene expression of *DR4* and *DR5* was upregulated in the BCR-ABL-transfected cells compared with control TF1 cells, which was abrogated by imatinib treatment (Figure 4b). Cell surface expression of DR4 and DR5 was also upregulated in the BCR-ABL-transfected cells, and the upregulated expression of DR5, but not DR4, returned to the control level by imatinib treatment (Figure 4c). In the absence of granulocyte/macrophage-colony stimulating factor, basal gene expression of *DR4* and *DR5* was at a low level in control cells (Figure 4d), but it was similarly upregulated in the BCR-ABL-transfected cells, which was abrogated by imatinib. Cell surface expression of DR4, but not DR5, was upregulated in the BCR-ABL-transfected cells (Figure 4e), and imatinib abrogated the BCR-ABL-induced upregulation of DR4.

The MAPK pathway is involved in DR4/DR5 expression in Ph(+) leukemia cells

Analysis of the BCR-ABL-transfected TF1 cells indicated that not only BCR-ABL but also growth factor stimulation has a role in DR4 and DR5 expression. Consistently, Interleukin-6 efficiently supported the growth of imatinib-treated KOPM30 cells by activating the MAPK, PI3K and JAK/STAT pathways without reactivating BCR-ABL (Figure 5a), and it partially compensated the imatinib-induced downregulation of gene (Figure 5b) and cell surface expression (Figure 5c) of DR4 and DR5. Next, to identify the pathways critical for BCR-ABL-induced DR4 and DR5 expression in Ph(+) leukemia, we analyzed the effects of specific inhibitors for each downstream pathway of BCR-ABL in KOPM30 cells. U0126, an inhibitor of the MAPK pathway, and LY294002, an inhibitor of the PI3K pathway, but not SD1029, an inhibitor of the JAK/STAT pathway,

Figure 3. Impact of T315I mutation and effect of shRNA against *bcr-abl* on the DR4 and DR5 expression. (**a**) Imatinib-induced dephosphorylation of BCR-ABL in SU-Ph2 and SU/SR. Cells were incubated with imatinib for 2 h and harvested for immunoblotting. (**b** and **c**) Gene and cell surface expression of DR4 and DR5 in SU-Ph2 and SU/SR cells treated with imatinib. Cells cultured in the absence or presence of imatinib (0.5 μM) for (**c**) 12 and (**b** and **c**) 24 h were analyzed for (**b**) *DR4* and *DR5* gene expression by real-time RT–PCR using *GAPDH* as an internal control and (**c**) cell surface expression of DR4 and DR5 by flow cytometry. Relative gene expression levels are indicated with error bars in triplicate experiments, and RFI is indicated in each box. Asterisk indicates significant difference ($P<0.01$, *t*-test) between SU-Ph2 and SU/SR. (**d**) Expression of BCR-ABL in lentivirus-infected KOPM30 cells. Twenty-four hours after infection, the GFP-positive population was analyzed by Western blotting using β-actin as an internal control. Relative expression levels with error bars are indicated in the right panel in triplicate experiments. Asterisk indicates significant difference ($P<0.01$, *t*-test) compared with control. (**e**) Time course of changes in the percentage of the GFP-positive population in lentivirus-infected KOPM30 cells. KOPM30 cells were infected with control or two types of shRNA-containing lentivirus vectors, and GFP-positive populations were monitored by flow cytometry. Percentages of GFP-positive population in the control, shRNA no. 1, or shRNA no. 3 lentivirus-transfected cells are indicated with error bars in triplicate infections. (**f** and **g**) Gene expression of *bcr-abl*, *DR4* and *DR5* in lentivirus-infected KOPM30 cells. Forty-eight hours after infection, gene expression of *bcr-abl* (**f**) and *DR4* and *DR5* (**g**) in GFP-positive population was analyzed by real-time RT–PCR using *GAPDH* as an internal control. Relative gene expression levels are indicated with error bars in triplicate experiments. Asterisk indicates significant difference ($P<0.01$, *t*-test) compared with control. (**h**) Cell surface expression of DR4 and DR5 in the GFP-positive population of lentivirus-infected KOPM30 cells cultured in the absence or presence of Q-VD-OPh. Cell surface expression of DR4 and DR5 on GFP-positive populations in control or shRNA no. 3 lentivirus-transfected KOPM30 cells cultured in the absence or presence of Q-VD-OPh (10 μM) for 48 h was analyzed by flow cytometry. Percentages of positive cells in triplicate infection are indicated in the lower panel with error bars. Asterisk indicates significant difference ($P<0.01$, *t*-test) compared with control.

downregulated gene (Figure 5d) and cell surface expression (Figure 5e) of DR4 and DR5. To further verify the involvement of the MAPK pathway, short interfering RNA (siRNA) against *ERK1* was introduced into KOPM30 cells using electroporation. Gene and protein expression of ERK1 were markedly lower by the introduction of siRNA against *ERK1*, but not by non-target siRNA (control), 30 and 36 h after transfection, respectively (Figures 5f and g). Gene and cell-surface expression of DR4 and DR5 were downregulated 36 h after transfection of siRNA against *ERK1* (Figures 5f and h). Next, to further verify the involvement of the

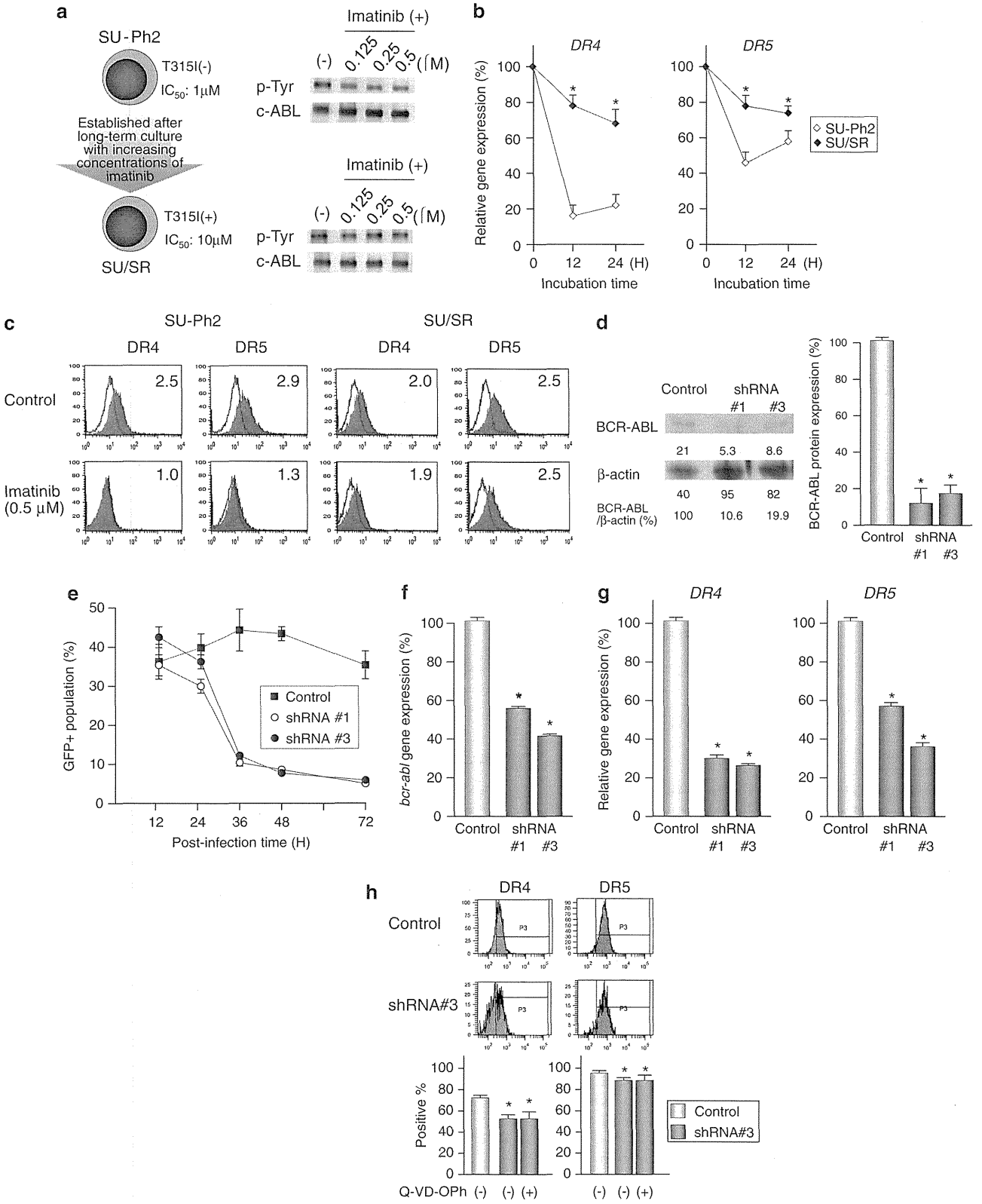

Figure 3. For caption see page 1673.

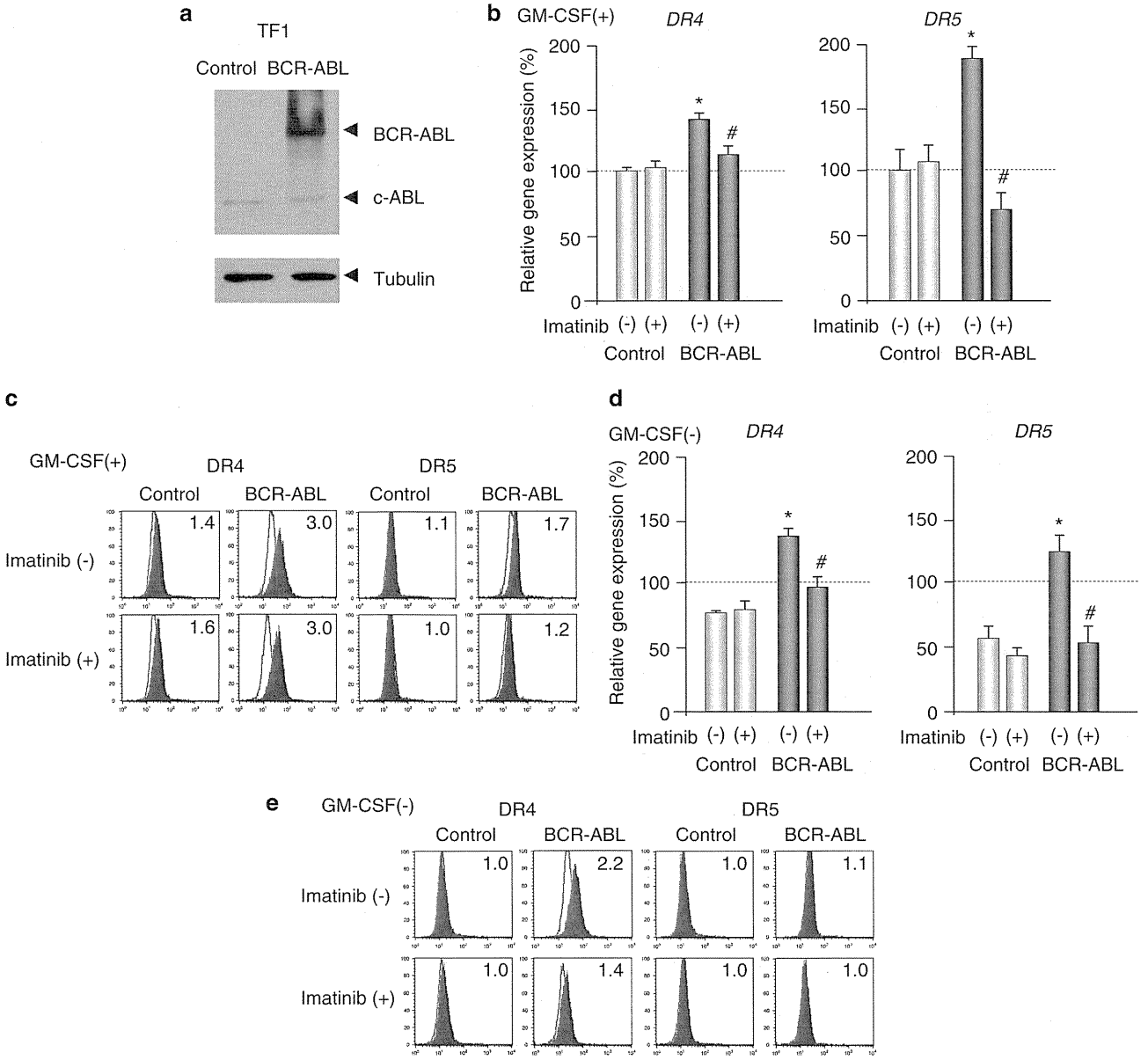

Figure 4. DR4 and DR5 expression in BCR-ABL-transfected TF1 cells. (**a**) BCR-ABL expression in transfected TF1 cells. (**b**–**e**) Gene and cell surface expression of DR4 and DR5 in parental and BCR-ABL-transfected TF1 cells cultured in the presence or absence of granulocyte/macrophage-colony stimulating factor (GM-CSF). Cells cultured in the presence (**b** and **c**) or absence (**d** and **e**) of GM-CSF for 24 h were analyzed for *DR4* and *DR5* gene expression by real-time RT–PCR using *GAPDH* as an internal control (**b** and **d**), and were analyzed for DR4 and DR5 cell surface expression by flow cytometry (**c** and **e**). Relative gene expression (**b** and **d**) is indicated with error bars in triplicate experiments, and a representative RFI is indicated in **c** and **e**. Asterisk indicates significant difference ($P<0.01$, *t*-test) compared with control and # indicates significant difference between imatinib (−) and imatinib (+) of BCR-ABL-transfected cells.

PI3K pathway, the effects of two representative inhibitors of the PI3K pathway, wortmannin and AS605240, on DR4 and DR5 expression in KOPM30 cells were also tested. However, both wortmannin (up to 100 nM) and AS605249 (up to 10 μM) failed to downregulate cell surface expression of DR4 and DR5 (data not shown). These observations indicated that at least the MAPK pathway is involved in DR4 and DR5 expression in KOPM30 cells.

Imatinib impairs the anti-leukemic activity of TRAIL in Ph(+) leukemia cells

Because imatinib downregulates cell surface expression of DR4 and DR5 in Ph(+) leukemia cells, it is assumed that the pro-apoptotic activity of TRAIL against Ph(+) leukemia cells may be functionally impaired by pretreatment with imatinib. Thus, we analyzed the effect of imatinib on the sensitivity of Ph(+) leukemia cells to rhs TRAIL under two conditions: (1) cells were pretreated with imatinib for 12 h and subsequently exposed to rhs TRAIL in the presence of imatinib for an additional 12 h and (2) cells were simultaneously exposed to rhs TRAIL and imatinib for 12 h. In KOPM30 cells, the pro-apoptotic activity of rhs TRAIL was highly impaired by pretreatment with imatinib (0.5 μM), while it was maintained by simultaneous treatment with imatinib (Figures 6a and b). Imatinib pretreatment impaired the pro-apoptotic activity of TRAIL at 0.125 μM (Figure 6c), and reached a plateau at 0.25 μM that was maintained until 1.0 μM. In contrast, in KOPM28

cells, despite of its high sensitivity to the anti-leukemic activity of imatinib,[25] rhs TRAIL-induced cell death was rather enhanced by imatinib pretreatment (Figure 6b) in a dose-dependent manner (Figure 6c). To test the involvement of molecules that make up the death-inducing signaling complex and its downstream pathway in the different responses between KOPM28 and KOPM30, we performed Western blot analysis of these molecules in imatinib-treated KOPM28 and KOPM30 (Figure 6d). In KOPM28, imatinib downregulated FLIP$_S$, an anti-apoptotic molecule as a negative regulator of caspase 8, but did not affect procaspase 8, FADD,

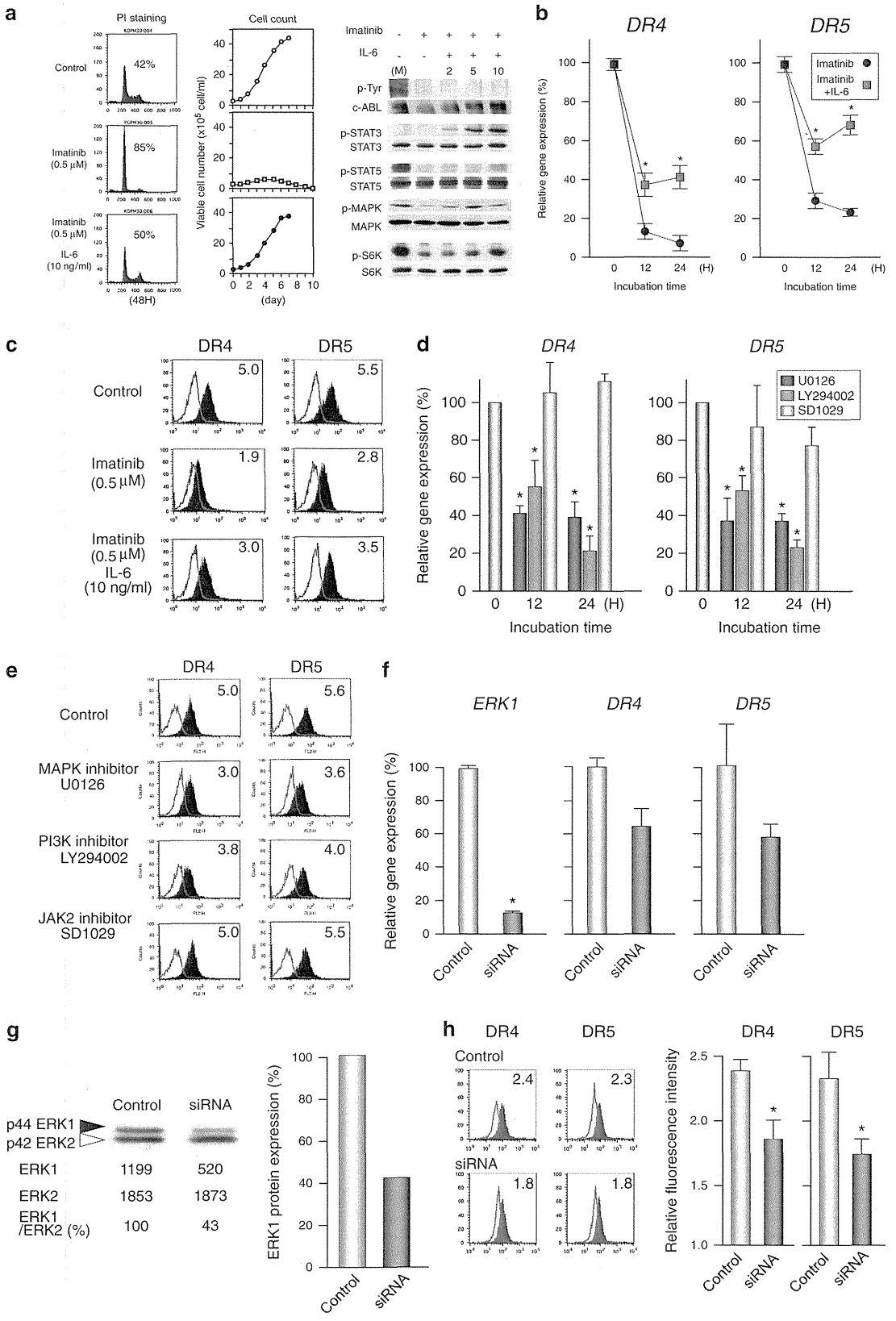

FLIP-$_L$, Bid, c-IAP1 and XIAP. In KOPM30, imatinib downregulated anti-apoptotic molecules such as FLIP-$_S$, c-IAP1 and c-IAP2, and only upregulated anti-apoptotic FLIP-$_L$. As summarized in Figure 6d, imatinib pretreatment at 0.5 μM significantly impaired sensitivity to the pro-apoptotic activity of rhs TRAIL in six out of the seven TRAIL-sensitive Ph(+) leukemia cell lines except for KOPM28. Of note, imatinib pretreatment of SU/SR cells, in which DR4 and DR5 expression was not downregulated due to the T315I mutation (Figure 3c),[29] did not lead to impaired TRAIL sensitivity, whereas imatinib pretreatment of parental SU-Ph2 cells led to substantially impaired TRAIL sensitivity (Figure 6e). We also tested the effect of imatinib pretreatment on the pro-apoptotic activity of rhs TRAIL using the primary sample from the Ph(+) ALL patient whose relative fluorescence intensity of DR4 and DR5 was downregulated from 4.0 and 4.5 to 2.0 and 2.5 by imatinib, respectively (Figure 2e), and confirmed that pretreatment of the sample with imatinib significantly reduced the sensitivity to rhs TRAIL (% viability improved from 56.6 ± 4.6 to 69.2 ± 3.2%, $P = 0.0003$ paired *t*-test) by trypan-blue exclusion assay (Figure 6f).

DISCUSSION

In the present study, we showed that imatinib specifically downregulated DR4 and DR5 expression in cell lines and clinical samples of Ph1-positive leukemia. In addition to imatinib, not only second-generation TKIs, including dasatinib and nilotinib, but also shRNA against *bcr-abl* downregulated DR4 and DR5 expression in Ph(+) leukemia cells. Moreover, transfection of *bcr-abl* into a Ph(−) leukemia cell line induced DR4 and DR5 expression that was abrogated by imatinib treatment. These observations clearly demonstrate that BCR-ABL has an important role in DR4 and DR5 expression in Ph(+) leukemia cells (Figure 7). BCR-ABL promotes growth and survival of Ph(+) leukemia cells through activation of the MAPK, PI3K and JAK/STAT pathways that are usually under control of growth factor stimulation.[3] Among these signaling pathways, the present study demonstrated that at least the MAPK pathway is involved in BCR-ABL-mediated DR4 and DR5 expression. That an oncogenic fusion product derived from chromosomal translocation is implicated in DR4 and DR5 expression on leukemia cells is a unique finding and provides new insight into the mechanisms of the tumor-specific cytotoxic activities of TRAIL.

Because it has been reported that TRAIL has a role in innate immunity for immune surveillance against tumor development,[18–20,22] our findings suggest that BCR-ABL sensitizes leukemia cells (or pre-leukemia cells) to innate immunity by upregulating DR4 and DR5 expression. This is a potentially paradoxical finding in that an oncogenic fusion protein indirectly suppresses expansion of leukemia cells. In this scenario, the chemical carcinogen methylcholanthrene (MCA)-induced mouse sarcoma model[20] may be worth noting: neutralization of endogenous TRAIL by anti-TRAIL antibody promoted development of sarcomas in mice treated with low-dose MCA but not significantly in mice treated with high-dose MCA. In this model, it was noted that high-dose MCA preferentially generated TRAIL-sensitive sarcomas, whereas low-dose MCA generated TRAIL-resistant sarcomas, suggesting that endogenous TRAIL-mediated immune surveillance could be overwhelmed by the emergence of high-potential tumors.[20] This experimental observation may be relevant to our paradoxical finding that Ph(+) leukemia cells show a clinically aggressive feature and poor therapeutic outcome upon chemotherapy despite of their sensitivity to TRAIL.

In addition to BCR-ABL, some other regulatory mechanisms also involve in DR4 and DR5 expression of Ph(+) leukemia cells. This assumption was supported by following two observations: (1) downreglation of DR4/DR5 expression by TKIs and siRNA against *bcr-abl* was partial in most of leukemia cell lines (e.c. KOPM28) and primary samples from Ph(+) ALL patients and (2) DR4 and DR5 expression was marginal in some Ph(+) leukemia cell lines (e.c. KOPN55bi) and primary samples from Ph(+) ALL patients. These mechanisms may include baseline activity of transcription factors and silencing by methylation of *DR4* and *DR5* gene promoter.[30] Thus, identification of these mechanisms that regulate DR4 and DR5 expression in Ph(+) leukemia cells cooperatively or independent with BCR-ABL is helpful to sensitize Ph(+) leukemia cells to pro-apoptotic activity of TRAIL.[27]

In most of the Ph(+) leukemia cell lines, pretreatment with imatinib reduced their sensitivity to rhs TRAIL. In contrast, pretreatment of KOPM28 with imatinib moderately sensitized the cells to rhs TRAIL. Moreover, Nimmanapalli *et al.*[31] previously reported that cotreatment with imatinib and rhs TRAIL induced apoptosis of K562 cells. Although these findings were potentially contrary to each other, there are several aspects that need to be considered. First, in the previous report by Nimmanapalli *et al.*,[31] K562 cells were simultaneously treated with imatinib and rhs TRAIL. When cells were simultaneously treated with imatinib and rhs TRAIL in the present study, imatinib did not reduce sensitivity to rhs TRAIL, if not sensitized. Second, as discussed above, there were some residual expressions of DR4 and DR5 after imatinib treatment. In this aspect, residual cell surface expression level of DR5 on KOPM28 was still higher than the cell surface expression levels on most of the other untreated Ph(+) cell lines (Figure 2c).

Figure 5. Effect of interleukin-6 (IL-6) and the signaling pathway inhibitors on DR4 and DR5 expression. (**a**) Effect of IL-6 on cell cycling, cell growth and phosphorylation of signaling molecules of imatinib-treated KOPM30 cells. For cell cycling and cell growth analysis, cells were cultured in the presence or absence of imatinib (0.5 μM) or both IL-6 (10 ng/ml) and imatinib. Propidium iodide (PI) staining was performed by flow cytometry after 48 h incubation, and viable cell number was determined by trypan-blue exclusion assay. All the data on cell growth are presented as the mean of triplicate samples. Standard errors were always <10% (not shown). For immunoblotting, cells were incubated with imatinib for 2 h in the presence of imatinib at 0.5 μM in serum-free medium, subsequently stimulated by IL-6 at 10 ng/ml for 2, 5 and 10 min and harvested for analysis. (**b** and **c**) Gene and cell surface expression of DR4 and DR5 in KOPM30 cells treated with imatinib in the presence or absence of IL-6. Cells cultured with imatinib (0.5 μM) in the absence or presence of IL-6 (10 ng/ml) for (**b**) 12 and (**b** and **c**) 24 h were analyzed for (**b**) *DR4* and *DR5* gene expression by real-time RT–PCR using *GAPDH* as an internal control and (**c**) cell surface expression of DR4 and DR5 by flow cytometry. Relative gene expression levels are indicated with error bars in triplicate experiments, and RFI is indicated in each box. Asterisk indicates significant difference ($P < 0.01$, *t*-test) between IL-6 (−) and IL-6 (+). (**d** and **e**) Gene and cell surface expression of DR4 and DR5 in KOPM30 cells treated with inhibitors of the MAPK, PI3K and JAK/STAT pathways. Cells cultured in the absence or presence of U0126, an inhibitor of the MAPK pathway, LY294002, an inhibitor of the PI3K pathway, or SD1029, an inhibitor of the JAK/STAT pathway for (**d**) 12 and (**d** and **e**) 24 h were analyzed for (**d**) *DR4* and *DR5* gene expression by real-time RT–PCR using *GAPDH* as an internal control and (**e**) cell surface expression of DR4 and DR5 by flow cytometry. Relative gene expression levels are indicated with error bars in triplicate experiments, and RFI is indicated in each box. Asterisk indicates significant difference ($P < 0.01$, *t*-test) compared with time 0. (**f**–**h**) Effect of siRNA against *ERK1* on cell surface expression of DR4 and DR5 in KOPM30 cells. After 30 and 36 h transfection of siRNA against *ERK1* or non-target siRNA, KOPM30 cells were analyzed for gene expression of ERK1, DR4 and DR5 in triplicate (**f**) and relative protein expression of ERK1 to ERK2 (**g**), respectively. Cell surface expression of DR4 and DR5 was analyzed in triplicate 36 h after transfection (**h**). Asterisk indicates statistically significant difference ($P < 0.05$) in *t*-test.

Third, the effect of imatinib on death-inducing signaling complex and its downstream pathways must be considered. In fact, imatinib treatment of KOPM28 and KOPM30 induced some changes in expression of molecules involved in death-inducing signaling complex formation and its dowmnstream pathway (Figure 6d). In KOPM30, most of those changes were down-regulation of anti-apoptotic molecules such as FLIP-$_S$, c-IAP1 and c-IAP2 except for upregulation of XIAP, suggesting that down-regulation of DR4 and DR5 rather than changes in these molecules might be involved in the reduction of rhs TRAIL sensitivity. In

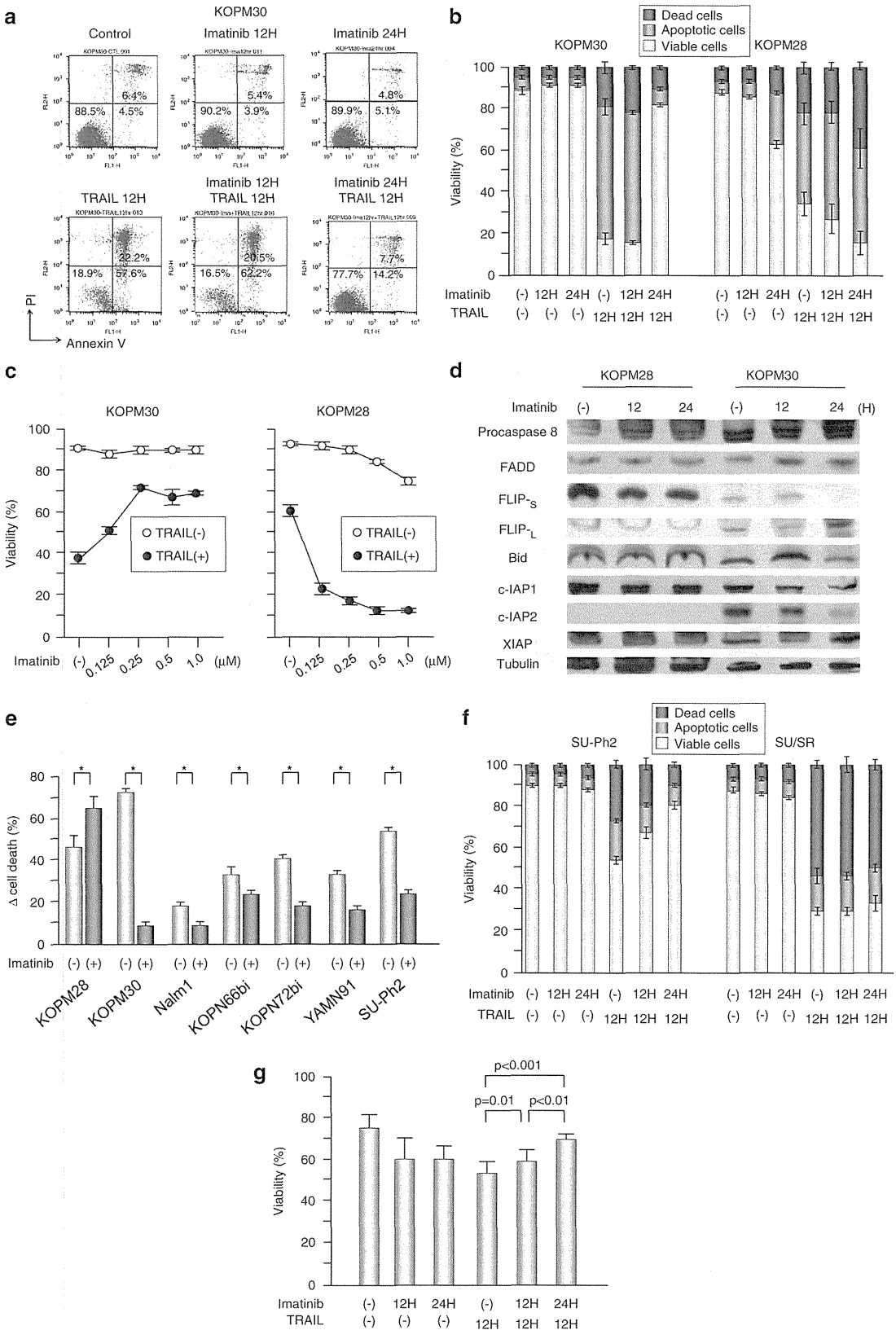

KOPM28, the expression level of FLIP-$_L$ was relatively high and was downregulated by imatinib, suggesting that the combination of residual DR5 expression and FLIP-$_L$ downregulation might be involved in TRAIL sensitivity.

From the clinical point of view, our finding that *in vitro* pretreatment of Ph(+) leukemia cells with imatinib reduced their sensitivity to the pro-apoptotic activity of rhs TRAIL in most cell lines is potentially important. Because imatinib is now widely used for prophylaxis of relapse as well as controlling hematological relapse after allo-SCT,[12,32–34] our findings suggested the possibility that in some patients, but not in all patients, imatinib treatment might partially attenuate the *in vivo* activity of cytotoxic T lymphocytes and natural killer cells against Ph(+) leukemia cells that is mediated by the TRAIL/death receptor interaction. In this context, however, we also showed *in vitro* that, when Ph(+) leukemia cells were simultaneously treated with imatinib and rhs TRAIL, imatinib marginally impaired the pro-apoptotic activity of rhs TRAIL. Moreover, although downregulation of DR4 and DR5 expression by imatinib was observed in most of DR4/DR5-positive primary samples from Ph(+) ALL patients, attenuation of pro-apoptotic activity of rhs TRAIL was rather restrictive. These observations suggest that the risk of an attenuated GVL effect by imatinib after allo-SCT would be substantially minimal if any. Indeed, several clinical studies reported the benefit of combination of imatinb and donor lymphocyte infusion in treatment of relapsed CML and Ph(+) ALL patients after allo-SCT.[35–37] Further *in vivo* studies are required to examine the effect of imatinib on TRAIL-mediated cellular immunity against Ph(+) leukemia.

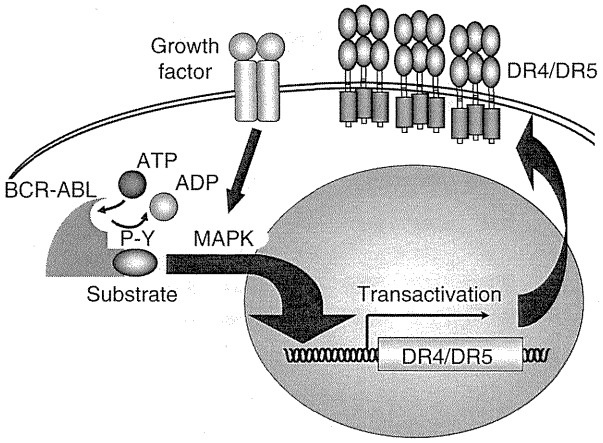

Figure 7. Schematic representation of BCR-ABL-induced DR4/DR5 expression in Ph(+) leukemia cells.

MATERIALS AND METHODS

Leukemia cell lines

KOPM28, KOPM53, Nalm1, K562 and KOPN55bi were established from patients with CML-BC; KOPN57bi, KOPN66bi, KOPN72bi and YAMN91 from patients with Ph(+) ALL rearranged in minor *bcr*;[25] YAMN73 from a patient with Ph(+) ALL expressing the abl exon 2-spliced BCR-ABL (203 kd) protein;[38] and KOPM30 and KOPN30bi from the same patient at different stages of the disease rearranged in minor *bcr*.[25] SU-Ph2 is an imatinib-sensitive cell line with double *BCR-ABL* fusion signals in fluorescence *in situ* hybridization analysis established from a patient with Ph(+) ALL, and SU/SR is an imatinib-resistant subline of SU-Ph2 obtained after long-term culture with increasing concentrations of imatinib.[29] As Ph(−) leukemia cell lines, Nalm6, a B-precursor ALL cell line, and Reh, a B-precursor ALL cell line with t(12;21), were used. All cell lines were maintained in RPMI 1640 medium supplemented with 10% fetal calf serum.

Clinical samples

Leukemia cells were isolated from bone marrow or peripheral blood samples (blasts >90%) of six Ph(+) ALL patients. Two samples were obtained at diagnosis and four samples were obtained at relapse. All of the four relapsed patients had not been treated with imatinib before. Mononuclear cells separated by Ficoll-Hypaque density centrifugation were stored in liquid nitrogen and used for experiments. Patients' sample analysis was approved by the ethical review board of University of Yamanashi.

Reagents

Imatinib mesylate and nilotinib were kindly provided by Novartis Pharmaceuticals (Basel, Switzerland) and dissolved in dimethyl sulfoxide. Q-VD-OPh, SD1029, U0126 and LY294002 were purchased from Calbiochem (Darmstadt, Germany) and dissolved in dimethyl sulfoxide. Recombinant human interleukin-6 was kindly provided by Kyowa Hakko Kirin (Tokyo, Japan).

Western blot analysis

Cell lines were transferred to serum-free D-MEM/F12 medium and treated with different concentration of imatinib for 2 h. The harvested cells were treated with 1 mM of AEBSF, hydrochloric acid (4-(2-Aminoethyl) benzensulfonylfluoride, HCl) (Calbiochem) for 10 min on ice, and then solubilized

Figure 6. Effect of imatinib treatment on the pro-apoptotic activity of rhs TRAIL against Ph(+) leukemia cells. (**a** and **b**) Pro-apoptotic activity of rhs TRAIL on KOPM30 and KOPM28 pretreated with imatinib. Cells that have been pretreated with or without imatinib at 0.5 μM for 12 h were further incubated in the absence or presence of 100 ng/ml of rhs TRAIL for 12 h, or cells were cultured in the absence or presence of 100 ng/ml of rhs TRAIL with or without imatinib (0.5 μM) for 12 h. Cell death was monitored by annexin V/PI staining. (**a**) Percentages of viable (annexin V (−) and PI (−)), apoptotic (annexin V (+) and PI (−)) and dead (annexin V (+) and PI (+)) cells are indicated in each box. (**b**) Mean percentages of viable, apoptotic and dead cells in triplicated analysis of KOPM30 and KOPM28 are indicated with error bars. (**c**) Dose effect of imatinib pretreatment on the pro-apoptotic activity of rhs TRAIL against KOPM30 and KOPM28. Cells that have been pretreated with imatinib at different concentrations for 12 h were further incubated in the absence or presence of 100 ng/ml of rhs TRAIL for 12 h. Cell death was monitored by annexin V/PI staining. Mean percentages of viable cells in triplicated analysis are indicated with error bars. (**d**) Effect of imatinib on the expression of molecules involved in death-inducing signaling complex formation and its downstream pathway. Western blotting was performed in KOPM28 and KOPM30 cells treated with imatinib (0.5 μM) for the indicated periods of time for procaspase 8, FLIP-$_L$, FLIP-$_S$, FADD, Bid, c-IAP1, c-IAP2 and XIAP, as well as tubulin as an internal control. (**e**) Effect of imatinib pretreatment on the pro-apoptotic activity of rhs TRAIL in Ph(+) leukemia cell lines. Cells that have been pretreated with or without imatinib at 0.5 μM for 12 h were further incubated in the presence of 100 ng/ml of rhs TRAIL for 12 h. Cell death was monitored by annexin V/PI staining. Mean Δ in cell death percentages (increases in percentages of apoptotic and dead cells by treatment with rhs TRAIL) in triplicated analysis are indicated with error bars, and asterisks indicate statistically significant difference in TRAIL-sensitivities between cells pretreated with and without imatinib by paired *t*-test ($P<0.05$). (**f**) Pro-apoptotic activity of rhs TRAIL on SU-Ph2 and SU/SR pretreated with imatinib. Cells that have been pretreated with or without imatinib at 0.5 μM for 12 h were further incubated in the absence or presence of 100 ng/ml of rhs TRAIL for 12 h, or cells were cultured in the absence or presence of 100 ng/ml of rhs TRAIL with or without imatinib (0.5 μM) for 12 h. Cell death was monitored by annexin V/PI staining. Mean percentages of viable, apoptotic and dead cells in triplicated analysis are indicated with error bars. (**g**) Pro-apoptotic activity of rhs TRAIL on primary sample pretreated with imatinib. Cells that have been pretreated with or without imatinib at 0.5 μM for 12 h were further incubated in the absence or presence of 100 ng/ml of rhs TRAIL for 24 h, or cells were cultured in the absence or presence of 100 ng/ml of rhs TRAIL with or without imatinib (0.5 μM) for 24 h. Viability was monitored by trypan-blue exclusion assay. Mean percentages of viable cells in triplicated analysis are indicated with error bars.

in lysis buffer (50 mM Tris-HCl, pH 7.5, 150 mM NaCl, 1% Nonidet P-40, 5 mM EDTA, 0.05% NaN_3, 1 mM phenylmethylsulfonyl fluoride and 100 μM sodium vanadate). The lysates were separated on a sodium dodecyl sulfate-polyacrylamide gel under reducing conditions and then transferred to a nitrocellulose membrane. The membrane was incubated with the first antibody at 4 °C overnight and then with horseradish peroxidase-labeled second antibody at room temperature for 1 h. The bands were developed using an enhanced chemiluminescence detection kit (Amersham Japan, Tokyo, Japan). As the first antibodies, anti-phospho-tyrosine monoclonal antibody (mAb) was purchased from Upstate Biotechnology (Lake Placid, NY, USA), anti-c-ABL mAb from Pharmingen (San Diego, CA, USA), anti-STAT5 mAb from Transduction Laboratories (Lexington, KY, USA), anti-p44/42 MAPK, anti-p70 S6 kinase (S6K), anti-phospho-STAT5 (Tyr694), anti-phospho-p44/42 MAPK (Thr202/Tyr204) and anti-phospho-p70 S6K (Thr421/Ser424) rabbit sera from New England BioLabs (Beverly, MA, USA), anti-Bid rabbit serum from Cell Signaling Technology (Danvers, MA, USA), anti-c-IAP1 and anti-c-IAP2 Bid rabbit sera from R&D systems (Minneapolis, MN, USA), anti-caspase 8 mAb from MBL (Nagoya, Japan), anti-FLIP-$_{S/L}$ mAb from Santa Cruz Biotechnology (Santa Cruz, CA, USA), anti-FADD and anti-XIAP mAbs from BD Biosciences (San Jose, CA, USA) and anti-β actin mAb from Sigma-Aldrich (St Louis, MO, USA). Horseradish peroxidase-conjugated anti-mouse IgG and anti-rabbit IgG were purchased from MBL.

Cell surface expression of TRAIL receptors

mAbs specific for DR4 and DR5 were originally generated, and the specificity of each mAb was confirmed against baby hamster kidney cell lines stably transfected with respective human TRAIL receptors cDNAs as previously reported.[25] Cells (1×10^6 cells) were incubated with 1 μg of biotinylated control mouse IgG1 or mAb on ice for 30 min. After washing, the cells were incubated with phycoerythrin-conjugated streptavidin (Biomeda, Foster City, CA, USA) on ice for 30 min and then analyzed by flow cytometry (FACSCalibur; BD Biosciences). The relative fluorescence intensity was calculated as the ratio of the mean fluorescence intensity of specific staining to that of control staining.

Real-time PCR analysis

Total RNA was extracted using the Trizol reagent (Invitrogen, Carlsbad, CA, USA). Reverse transcription was performed with random hexamer (Amersham Bioscience, GE Healthcare Life Sciences, Little Chalfont, UK) and Superscript II reverse transcriptase (Invitrogen), and obtained cDNA was then incubated with 1 ml of RNase (Invitrogen) at 37 °C for 20 min. For quantitative real-time PCR of *DR4*, *DR5* and *ERK1* transcripts, triplicated samples containing 9 μl of cDNA with 10 μl of Taqman Universal PCR Master Mix (Applied Biosystems, Foster City, CA, USA) and 1 μl of 20 × Assays-on-demand Gene Expression Product (DR4, Hs 00269492_m1; DR5, Hs 00366272_m1; ERK1, Hs 00385075_m1; Applied Biosystems) were pre-incubated at 50 °C for 2 min and subsequently at 95 °C for 10 min. Amplification was obtained by 40 cycles of reaction at 95 °C for 15 s and 60 °C for 1 min. Fluorescence data were quantitatively analyzed on ABI Prism 7500 Sequence Detection System (Applied Biosystems). Nalm1 was used for positive control. As an internal control, quantitative real-time PCR for *GAPDH* (Hs 99999905_m1; Applied Biosystems) was performed.

Cytotoxic activity assays

Rhs TRAIL (Killer TRAIL), which is composed of the extracellular domain of human TRAIL fused at the N-terminus to a linker peptide and His-tag was purchased from Alexis Biochemicals (San Diego, CA, USA). To detect the early apoptotic event, cells (4×10^5 cells/ml) were cultured in the absence or presence of rhs TRAIL (100 ng/ml), harvested at 12 h, stained with fluorescein isothiocyanate-conjugated annexin V (MBL) and propidium iodide and analyzed by flow cytometry (FACSCalibur). For clinical sample, trypan-blue exclusion assay was performed.

Reporter assays

A −820/−2 fragment of the *DR4* gene generated using PCR was cloned into the pGL3-basic vector (Promega, Madison, WI, USA) and subjected to nucleotide sequence analysis.[30] The *Pst*/*Mlu*I fragment of the *DR5* gene cloned into the pGL3-basic vector was a gift from T Sakai (Kyoto Prefectural University of Medicine, Japan).[39] pRL-TK vector (Promega) was used to monitor the transfection efficiency. Transfection was performed in triplicate by lipofectamine (Invitrogen) following the manufacturer's instruction. After 24 h transfection, aliquots of cells were cultured in the presence or absence of 0.2 μM of imatinib for 24 h, and the cells were finally harvested for assay 48 h after transfection. Activities of firefly and *Renilla* luciferases were measured sequentially using Dual-Luciferase reporter assay system (Promega).

Lentivirus shRNA/siRNA expression vectors and infection

pLL3.7 lentiviral vector was engineered to produce shRNAs under the control of mouse U6 promoter and co-express GFP as a reporter gene by CMV-GFP expression cassette.[40] siRNA-target sequences were designed to be homologous to the p190 *bcr-abl* cDNA sequence, and oligonucleotides were subcloned into pLL3.7. The selected sequences were submitted to BLAST search to assure that only *bcr-abl* was targeted. Among five sets of oligonucleotides containing siRNA-target sequences, the following two sets were selected for further analysis due to the specificity and efficiency: no. 1, 5′-TgggtcttaggctataatcaTTCAAGAGAtgattatagcctaagacccTTTTTTC-3′ (blunt-siRNA/sense hairpin-siRNA/antisense-polyA-*Xho*I/forward); no. 3, 5′-Tgattccatccagcaaatga**TTCAAGAGA**tcatttgctggatggaatcTTTTTTC-3′ (forward). The control vector contained the following ineffective sequence: 5′-TgcaatattacatatacgccTTCAAGAGAggcgtatatgtaatattgcTTTTTTC-3′ (forward). pLL3.7 shRNA vector or control vector was cotransfected with packaging vector into 293FT cells and the resulting supernatant was collected after 36 h.[41] Lentivirus was recovered after ultracentrifugation and infected to KOPM30 cells.

Introduction of siRNA using electroporation

siRNA against *ERK1* (s230180) and non-specific siRNA were purchased from Applied Biosystems. Introduction of siRNA into KOPM30 cells was performed using Neon Transfection System (Life Technologies, Carlsbad, CA, USA). Electroshock (pulse voltage, 1700 V; pulse width, 20 ms; pulse number, × 1) was performed using T-buffer, and cells were harvested for real-time reverse transcriptase PCR and immunoblotting or flow cytometric analysis 30 and 36 h after electroporation, respectively.

CONFLICT OF INTEREST

The authors declare no conflict of interest.

ACKNOWLEDGEMENTS

The authors thank technological supports by Masako Abe. This work was supported in part by research grants from the Ministry of Education, Science and Culture, Japan.

REFERENCES

1 Faderl S, Talpaz M, Estrov Z, O'Brien S, Kurzrock R, Kantarjian HM. The biology of chronic myeloid leukemia. *N Engl J Med* 1999; **341**: 164–172.
2 Hehlmann R, Hochhaus A, Baccarani M. European LeukemiaNet. Chronic myeloid leukaemia. *Lancet* 2007; **370**: 342–350.
3 Quintás-Cardama A, Cortes J. Molecular biology of bcr-abl1-positive chronic myeloid leukemia. *Blood* 2009; **113**: 1619–1630.
4 Preti HA, O'Brien S, Giralt S, Beran M, Pierce S, Kantarjian HM. Philadelphia-chromosome-positive adult acute lymphocytic leukemia: characteristics, treatment results, and prognosis in 41 patients. *Am J Med* 1994; **97**: 60–65.
5 Uckun FM, Nachman JB, Sather HN, Sensel MG, Kraft P, Steinherz PG *et al.* Clinical significance of Philadelphia chromosome positive pediatric acute lymphoblastic leukemia in the context of contemporary intensive therapies: a report from the Children's Cancer Group. *Cancer* 1998; **83**: 2030–2039.
6 Druker BJ, Tamura S, Buchdunger E, Ohno S, Segal GM, Fanning S *et al.* Effects of a selective inhibitor of the Abl tyrosine kinase on the growth of Bcr-Abl positive cells. *Nat Med* 1996; **2**: 561–566.
7 Druker BJ, Talpaz M, Resta DJ, Peng B, Buchdunger E, Ford JM *et al.* Efficacy and safety of a specific inhibitor of BCR-ABL tyrosine kinase in chronic myeloid leukemia. *N Engl J Med* 2001; **344**: 1031–1037.
8 Druker BJ, Sawyers CL, Kantarjian H, Resta DJ, Reese SF, Ford JM *et al.* Activity of a specific inhibitor of the BCR-ABL tyrosine kinase in the blastic crisis of chronic myeloid leukemia and acute lymphoblastic leukemia with the Philadelphia chromosome. *N Engl J Med* 2001; **344**: 1038–1042.
9 Jabbour E, Hochhaus A, Cortes J, La Rosée P, Kantarjian HM. Choosing the best treatment strategy for chronic myeloid leukemia patients resistant to imatinib: weighing the efficacy and safety of individual drugs with BCR-ABL mutations and patient history. *Leukemia* 2010; **24**: 6–12.

10 Jabbour E, Kantarjian H, O'Brien S, Shan J, Garcia-Manero G, Wierda W *et al.* Predictive factors for outcome and response in patients treated with second-generation tyrosine kinase inhibitors for chronic myeloid leukemia in chronic phase after imatinib failure. *Blood* 2011; **117**: 1822–1827.
11 Arico M, Valsecchi MG, Camitta B, Schrappe M, Chessells J, Baruchel A *et al.* Outcome of treatment in children with Philadelphia chromosome-positive acute lymphoblastic leukemia. *N Engl J Med* 2000; **342**: 998–1006.
12 Fielding AK. How I treat Philadelphia chromosome-positive acute lymphoblastic leukemia. *Blood* 2010; **116**: 3409–3417.
13 Kolb HJ, Schmid C, Barrett AJ, Schendel DJ. Graft-versus-leukemia reactions in allogeneic chimeras. *Blood* 2003; **103**: 767–776.
14 Kolb HJ. Graft-versus-leukemia effects of transplantation and donor lymphocytes. *Blood* 2008; **112**: 4371–4383.
15 Kagi D, Vignaux F, Ledermann B, Depraetere V, Nagata S, Hengartner H *et al.* Fas and perforin pathways as major mechanisms of T cell-mediated cytotoxicity. *Science* 1994; **265**: 528–530.
16 Lowin B, Hahne M, Mattmann C, Tschopp J. Cytolytic T-cell cytotoxicity is mediated through perforin and Fas lytic pathways. *Nature* 1994; **370**: 650–652.
17 Smyth MJ, Cretney E, Takeda K, Wiltrout RH, Sedger LM, Kayagaki N *et al.* Tumor necrosis factor-related apoptosis-inducing ligand (TRAIL) contributes to interferon gamma-dependent natural killer cell protection from tumor metastasis. *J Exp Med* 2001; **193**: 661–670.
18 Takeda K, Hayakawa Y, Smyth MJ, Kayagaki N, Yamaguchi N, Kakuta S *et al.* Involvement of tumor necrosis factor-related apoptosis-inducing ligand in surveillance of tumor metastasis by liver natural killer cells. *Nat Med* 2001; **7**: 94–100.
19 Cretney E, Takeda K, Yagita H, Glaccum M, Peschon JJ, Smyth MJ. Increased susceptibility to tumor initiation and metastasis in TNF-related apoptosis-inducing ligand-deficient mice. *J Immunol* 2002; **168**: 1356–1361.
20 Takeda K, Smyth MJ, Cretney E, Hayakawa Y, Kayagaki N, Yagita H *et al.* Critical role for tumor necrosis factor-related apoptosis-inducing ligand in immune surveillance against tumor development. *J Exp Med* 2002; **195**: 161–169.
21 Schmaltz C, Alpdogan O, Kappel BJ, Muriglan SJ, Rotolo JA, Ongchin J *et al.* T cells require TRAIL for optimal graft-versus-tumor activity. *Nat Med* 2002; **8**: 1433–1437.
22 Takeda K, Stagg J, Yagita H, Okumura K, Smyth MJ. Targeting death-inducing receptors in cancer therapy. *Oncogene* 2007; **26**: 3745–3757.
23 Pan G, O'Rourke K, Chinnaiyan AM, Gentz R, Ebner R, Ni J *et al.* The receptor for the cytotoxic ligand TRAIL. *Science* 1997; **276**: 111–113.
24 Pan G, Ni J, Wei YF, Yu G, Gentz R, Dixit VM. An antagonist decoy receptor and death domain-containing receptor for TRAIL. *Science* 1997; **277**: 815–821.
25 Uno K, Inukai T, Kayagaki N, Goi K, Sato H, Nemoto A *et al.* TNF-related apoptosis-inducing ligand (TRAIL) frequently induces apoptosis in Philadelphia chromosome-positive leukemia cells. *Blood* 2003; **101**: 3658–3667.
26 Gonzalvez F, Ashkenazi A. New insights into apoptosis signaling by Apo2L/TRAIL. *Oncogene* 2010; **29**: 4752–4765.
27 Zhang X, Inukai T, Akahane K, Hirose K, Kuroda I, Honna H *et al.* Endoplasmic reticulum stress inducers, but not imatinib, sensitize Philadelphia chromosome-positive leukemia cells to TRAIL-mediated apoptosis. *Leuk Res* 2011; **35**: 940–949.
28 Sheridan JP, Marsters SA, Pitti RM, Gurney A, Skubatch M, Baldwin D *et al.* Control of TRAIL-induced apoptosis by a family of signaling and decoy receptors. *Science* 1997; **277**: 818–821.
29 Hirase C, Maeda Y, Takai S, Kanamaru A. Hypersensitivity of Ph-positive lymphoid cell lines to rapamycin: possible clinical application of mTOR inhibitor. *Leuk Res* 2009; **33**: 450–459.
30 Akahane K, Inukai T, Zhang X, Hirose K, Kuroda I, Goi K *et al.* Resistance of T-cell acute lymphoblastic leukemia to tumor necrosis factor-related apoptosis-inducing ligand-mediated apoptosis. *Exp Hematol* 2010; **38**: 885–895.
31 Nimmanapalli R, Porosnicu M, Nguyen D, Worthington E, O'Bryan E, Perkins C *et al.* Cotreatment with STI-571 enhances tumor necrosis factor alpha-related apoptosis-inducing ligand (TRAIL or apo-2L)-induced apoptosis of Bcr-Abl-positive human acute leukemia cells. *Clin Cancer Res* 2001; **7**: 350–357.
32 Hess G, Bunjes D, Siegert W, Schwerdtfeger R, Ledderose G, Wassmann B *et al.* Sustained complete molecular remissions after treatment with imatinib-mesylate in patients with failure after allogeneic stem cell transplantation for chronic myelogenous leukemia: results of a prospective phase II open-label multicenter study. *J Clin Oncol* 2005; **23**: 7583–7593.
33 Carpenter PA, Snyder DS, Flowers ME, Sanders JE, Gooley TA, Martin PJ *et al.* Prophylactic administration of imatinib after hematopoietic cell transplantation for high-risk Philadelphia chromosome-positive leukemia. *Blood* 2007; **109**: 2791–2793.
34 Olavarria E, Siddique S, Griffiths MJ, Avery S, Byrne JL, Piper KP *et al.* Post-transplantation imatinib as a strategy to postpone the requirement for immunotherapy in patients undergoing reduced-intensity allografts for chronic myeloid leukemia. *Blood* 2007; **110**: 4614–4617.
35 Savani BN, Montero A, Kurlander R, Childs R, Hensel N, Barrett AJ. Imatinib synergizes with donor lymphocyte infusions to achieve rapid molecular remission of CML relapsing after allogeneic stem cell transplantation. *Bone Marrow Transplant* 2005; **36**: 1009–1015.
36 Yoshimitsu M, Fujiwara H, Ozaki A, Hamada H, Matsushita K, Arima N *et al.* Case of a patient with Philadelphia-chromosome-positive acute lymphoblastic leukemia relapsed after myeloablative allogeneic hematopoietic stem cell transplantation treated successfully with imatinib and sequential donor lymphocyte infusions. *Int J Hematol* 2008; **88**: 331–335.
37 Tiribelli M, Sperotto A, Candoni A, Simeone E, Buttignol S, Fanin R. Nilotinib and donor lymphocyte infusion in the treatment of Philadelphia-positive acute lymphoblastic leukemia (Ph+ ALL) relapsing after allogeneic stem cell transplantation and resistant to imatinib. *Leuk Res* 2009; **33**: 174–177.
38 Inukai T, Sugita K, Suzuki T, Ijima K, Goi K, Tezuka T *et al.* A novel 203 kD aberrant BCR-ABL product in a girl with Philadelphia chromosome positive acute lymphoblastic leukaemia. *Br J Haematol* 1993; **85**: 823–825.
39 Yoshida T, Maeda A, Tani N, Sakai T. Promoter structure and transcription initiation sites of the human death receptor 5/TRAIL-R2 gene. *FEBS Lett* 2001; **507**: 381–385.
40 Rubinson DA, Dillon CP, Kwiatkowski AV, Sievers C, Yang L, Kopinja J *et al.* A lentivirus-based system to functionally silence genes in primary mammalian cells, stem cells and transgenic mice by RNA interference. *Nat Genet* 2003; **33**: 401–406.
41 Hirose K, Inukai T, Kikuchi J, Furukawa Y, Ikawa T, Kawamoto H *et al.* Aberrant induction of LMO2 by the E2A-HLF chimeric transcription factor and its implication in leukemogenesis of B-precursor ALL with t(17;19). *Blood* 2010; **116**: 962–970.

Gene Regulation:

GENE REGULATION

The Novel Orally Active Proteasome Inhibitor K-7174 Exerts Anti-myeloma Activity *in Vitro* and *in Vivo* by Down-regulating the Expression of Class I Histone Deacetylases

Jiro Kikuchi, Satoshi Yamada, Daisuke Koyama, Taeko Wada, Masaharu Nobuyoshi, Tohru Izumi, Miyuki Akutsu, Yasuhiko Kano and Yusuke Furukawa

J. Biol. Chem. 2013, 288:25593-25602.
doi: 10.1074/jbc.M113.480574 originally published online July 22, 2013

THE JOURNAL OF BIOLOGICAL CHEMISTRY VOL. 288, NO. 35, pp. 25593–25602, August 30, 2013

The Novel Orally Active Proteasome Inhibitor K-7174 Exerts Anti-myeloma Activity *in Vitro* and *in Vivo* by Down-regulating the Expression of Class I Histone Deacetylases*

Received for publication, April 25, 2013, and in revised form, July 2, 2013 Published, JBC Papers in Press, July 22, 2013, DOI 10.1074/jbc.M113.480574

Jiro Kikuchi[‡], Satoshi Yamada[‡], Daisuke Koyama[‡], Taeko Wada[‡], Masaharu Nobuyoshi[‡], Tohru Izumi[§], Miyuki Akutsu[§], Yasuhiko Kano[§], and Yusuke Furukawa[‡1]

From the [‡]Division of Stem Cell Regulation, Center for Molecular Medicine, Jichi Medical University, Shimotsuke, Tochigi 329-0498 and the [§]Division of Hematology, Tochigi Cancer Center, Utsunomiya, Tochigi 320-0834, Japan

Background: Orally active proteasome inhibitors with novel mechanisms of action are in high clinical demand.
Results: K-7174, a homopiperazine derivative with a unique mode of proteasome inhibition, exhibits anti-myeloma effects via transcriptional repression of class I histone deacetylases.
Conclusion: K-7174 is an orally active proteasome inhibitor with a unique mechanism of action.
Significance: K-7174 may compensate for conventional proteasome inhibitors in cancer treatment.

Bortezomib therapy is now indispensable for multiple myeloma, but is associated with patient inconvenience due to intravenous injection and emerging drug resistance. The development of orally active proteasome inhibitors with distinct mechanisms of action is therefore eagerly awaited. Previously, we identified homopiperazine derivatives as a novel class of proteasome inhibitors with a different mode of proteasome binding from bortezomib. In this study, we show that K-7174, one of proteasome inhibitory homopiperazine derivatives, exhibits a therapeutic effect, which is stronger when administered orally than intravenously, without obvious side effects in a murine myeloma model. Moreover, K-7174 kills bortezomib-resistant myeloma cells carrying a β5-subunit mutation *in vivo* and primary cells from a patient resistant to bortezomib. K-7174 induces transcriptional repression of class I histone deacetylases (HDAC1, -2, and -3) via caspase-8-dependent degradation of Sp1, the most potent transactivator of class I HDAC genes. HDAC1 overexpression ameliorates the cytotoxic effect of K-7174 and abrogates histone hyperacetylation without affecting the accumulation of ubiquitinated proteins in K-7174-treated myeloma cells. Conversely, HDAC inhibitors enhance the activity of K-7174 with an increase in histone acetylation. These results suggest that class I HDACs are critical targets of K-7174-induced cytotoxicity. It is highly anticipated that K-7174 increases the tolerability and convenience of patients by oral administration and has the clinical utility in overcoming bortezomib resistance as a single agent or in combination with HDAC inhibitors.

Proteasome inhibition is now considered a unique and effective way to kill cancer cells that can tolerate conventional chemotherapy. Bortezomib is the first proteasome inhibitor (PI)[2] approved for clinical application, and is now used for the treatment of multiple myeloma (MM) and mantle cell lymphoma (1–3). Although bortezomib therapy is a major advance in clinical oncology, there are several problems to be resolved as soon as possible (4, 5). Among them, off-target toxicities, patient inconvenience due to intravenous administration, and the development of both intrinsic and acquired resistance to bortezomib are emerging problems.

The introduction of novel orally active PIs with distinct mechanisms of action from bortezomib is an effective way to circumvent these issues. Recently, several novel PIs have been developed and are now undergoing clinical trials (6). Although some compounds are orally available, most of them are peptide derivatives and act via similar mechanisms of action as does bortezomib (7–12). In addition, point mutations in the proteasome β5 subunit gene underlying bortezomib resistance have been reported (13–15). Therefore, we still intend to develop novel orally bioavailable PIs with distinct mechanisms of action from bortezomib.

K-7174 (*N*,*N*′-bis-(*E*)-[5-(3,4,5-trimethoxy-phenyl)-4-pentenyl]homopiperazine) is a homopiperazine-derived small molecular compound developed as an orally active agent *in vivo* (see Fig. 1*A* for chemical structure) (16, 17). In a previous study, we have shown that K-7174 inhibits all three catalytic subunits of 20 S proteasome by direct binding, whereas bortezomib mainly acts on the β5 subunit (18). However, it is still unclear whether K-7174 has anti-myeloma activity and its underlying mechanism is different from that of bortezomib. The initial rationale for the use of bortezomib was the inhibition of NF-κB

* This work was supported in part by the High-Tech Research Center Project for Private Universities, Matching Fund Subsidy from MEXT, a Grant-in-Aid for Scientific Research from JSPS (to J. K. and Y. F.), the Adaptable and Seamless Technology transfer Program (A-STEP) from JST, and research grants from Japan Leukemia Research Fund, Takeda Science Foundation, Kano Foundation, Mitsui Life Social Welfare Foundation, and Osaka Cancer Foundation (to J. K.).

[1] Winner of the Award in Aki's Memory from the International Myeloma Foundation Japan. To whom correspondence should be addressed. Tel.: 81-285-58-7400; Fax: 81-285-44-7501; E-mail: furuyu@jichi.ac.jp.

[2] The abbreviations used are: PI, proteasome inhibitor; HDAC, histone deacetylase; MM, multiple myeloma; MTT, 3-(4,5-dimethylthiazol-2-yl)-2,5-diphenyltetrazolium bromide; NOD/SCID, non-obese diabetic/severe combined immunodeficiency; PSMB5, proteasome β5-subunit; VCAM-1, vascular cell adhesion molecule-1; Z, benzyloxycarbonyl; fmk, fluoromethyl ketone; DMSO, dimethyl sulfoxide.

activity, since IκBα, which inactivates NF-κB, is a substrate of the proteasome complex (19). This scenario was challenged by the recent report of Hideshima *et al.* (20), in which bortezomib did not inactivate but rather activated the canonical NF-κB pathway in MM cells. Moreover, we have found that down-regulation of class I histone deacetylases (HDACs) is one of the major mechanisms of the cytotoxic action of bortezomib (21). It is likely that K-7174 exerts anti-myeloma action via similar mechanisms.

In this study, we demonstrated anti-myeloma activity of post-oral K-7174 and the utility in overcoming bortezomib resistance using a murine xenograft model. Moreover, we found that the cytotoxic activity of K-7174 largely depends on the expression levels of class I HDACs and the combination of K-7174 and HDAC inhibitors induces additive effects via the reduction of HDAC activity. These findings may provide a molecular basis and rationale for the use of K-7174 in myeloma treatment alone or in combination with HDAC inhibitors.

EXPERIMENTAL PROCEDURES

Cells and Cell Culture—We used 3 *bona fide* human MM cell lines, KMS12-BM, RPMI8226, and U266, in this study (22). These cell lines were purchased from the Health Science Research Resources Bank (Osaka, Japan). Primary CD138-positive MM cells were isolated from the bone marrow of patients at the time of the diagnostic procedure using the MACS system (Miltenyi Biotec, Gladbach, Germany). Informed consent was obtained in accordance with the Declaration of Helsinki, and the protocol was approved by the Institutional Review Board.

Drugs—The drugs used in this study and their sources are: K-7174 (Kowa, Tokyo, Japan), bortezomib (Millennium Pharmaceuticals, Cambridge, MA), 4-hydroperoxy cyclophosphamide (an active metabolite of cyclophosphamide) (Shionogi, Tokyo, Japan), melphalan (L-PAM) (Wako Biochemicals, Osaka, Japan), romidepsin (Gloucester Pharmaceuticals, Cambridge, MA), and vorinostat (Selleck Chemicals, Houston, TX).

Cell Proliferation Assay—Cell proliferation was measured by the 3-(4,5-dimethylthiazol-2-yl)-2,5-diphenyltetrazolium bromide (MTT) reduction assay using a Cell Counting Kit (Wako Biochemicals). Absorbance at 450 nm was analyzed with a microplate reader, and expressed as a percentage of the value of the corresponding untreated cells (23).

Assessment of Cell Death—Cells were washed with phosphate-buffered saline, and stained with allophycocyanin-conjugated annexin-V (Biovision, Mountain View, CA). Cell death/apoptosis was judged by annexin-V reactivity using a FACSaria flow cytometer (Becton Dickinson, Bedford, MA) as described previously (24).

Immunoblotting—Immunoblotting was carried out according to the standard method using the following antibodies: anti-acetyl histone H3 (Upstate Biotechnology/Millipore, Billerica, MA), anti-histone H3, anti-ubiquitin, anti-pro-caspase-8, -9, and -12, anti-HDAC2 (Cell Signaling Technology, Beverly, MA), anti-HDAC1 (Sigma), anti-HDAC3 (BD Transduction Laboratories, San Diego, CA), anti-CD138, anti-Sp1, and anti-GAPDH (Santa Cruz Biotechnology, Santa Cruz, CA) (21).

Semi-quantitative Reverse Transcription-Polymerase Chain Reaction (RT-PCR)—Total cellular RNA was isolated from 1 to 10×10^4 cells, reverse-transcribed into cDNA using SuperScript reverse transcriptase and oligo(dT) primers (Invitrogen), and subjected to subsequent semi-quantitative RT-PCR. Detailed information on the procedure was described previously (21).

Chromatin Immunoprecipitation Assays—We used the ChIP-IT Chromatin Immunoprecipitation Kit (Active Motif, Carlsbad, CA) to perform chromatin immunoprecipitation assays. In brief, cells were fixed with 1% formaldehyde at 37 °C for 5 min, and sonicated to obtain chromatin suspensions. After centrifugation, supernatants were incubated with antibodies of interest at 4 °C overnight. The mixture was then incubated with protein A-agarose beads at 4 °C for 1 h, and centrifuged to collect the beads. DNA fragments bound to the beads were purified with vigorous washing, and subjected to PCR as described previously (21).

Xenograft Murine Model—Cell suspensions in 100 μl of RPMI 1640 medium together with 100 μl of Matrigel basement membrane matrix (BD Biosciences) were inoculated subcutaneously into the right thigh of non-obese diabetic/severe combined immunodeficiency (NOD/SCID) mice (Charles River Laboratories, Wilmington, MA). Treatment was started after tumors were measurable (100–500 mm^3) as described previously (21). K-7174 was administered intraperitoneally or orally in a volume of 400 μl of solution containing 3% DMSO and 97% sterile 0.9% NaCl once daily at various doses for 2 weeks. Bortezomib was administered intravenously twice a week via the tail vein at 0.5 mg/kg for 2 weeks. The control group received the vehicle (3% DMSO in 0.9% NaCl) alone on the same schedule. Caliper measurements of the longest perpendicular tumor diameters were performed every alternate day to estimate tumor volume using the following formula: $4/3\pi \times (\text{width}/2)^2 \times (\text{length}/2)$, which represents the three-dimensional volume of an ellipse.

Establishment of Bortezomib-resistant MM Cell Lines—To confer bortezomib resistance to MM cells, we transduced with mutated *PSMB5* cDNA as described previously (18, 25). A mutation was inserted at nucleotide position 322 (G/A) by PCR-based site-directed mutagenesis. Wild-type and mutated *PSMB5* cDNAs were inserted into the lentiviral vector CSII-CMV-MCS-IRES-VENUS (kindly provided by Dr. Hiroyuki Miyoshi, RIKEN BioResource Center, Ibaraki, Japan) (26), and co-transfected into 293FT cells with packaging plasmids (Invitrogen) to produce infective lentiviruses in culture supernatants (27). RPMI8226 cells were infected by each viral supernatant for 24 h. We collected VENUS-positive cells by a FACSaria flow cytometer, seeded 1 cell/well in a 96-well plate to obtain single cell clones.

RESULTS

K-7174 Inhibits MM Cell Growth in Vitro—Following the demonstration of proteasome inhibitory action (18), we investigated whether K-7174 exerts anti-myeloma activities. First, we examined the cytotoxic effect of K-7174 on MM cell lines using MTT assays. K-7174 significantly inhibited the growth of three MM cell lines in a dose-dependent manner (Fig. 1B).

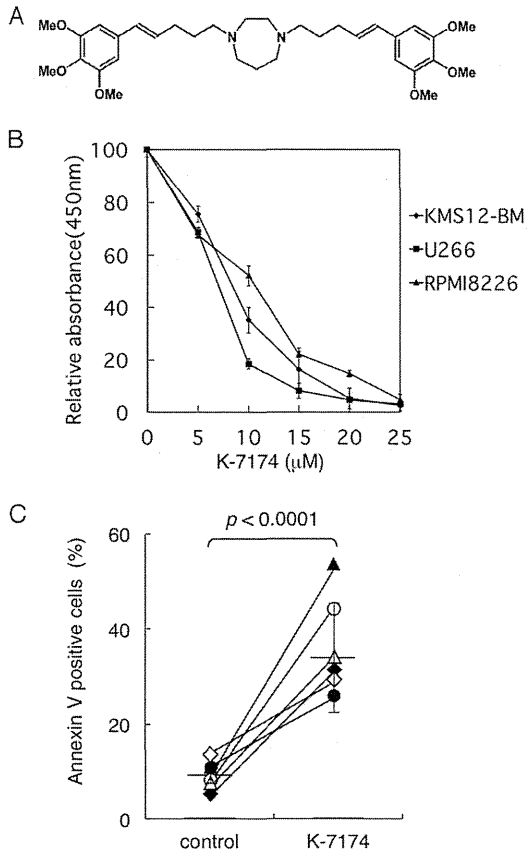

FIGURE 1. **Anti-myeloma activity of K-7174 *in vitro*.** *A*, chemical structure of K-7174. *B*, cell proliferation was measured by MTT assays after culturing MM cells with K-7174 for 72 h. Absorbance at 450 nm was analyzed with a microplate reader, and expressed as a percentage of the value of corresponding untreated cells. Panels show the dose-response curves of KMS12-BM (*closed diamond*), U266 (*closed square*), and RPMI8226 (*closed triangle*) cells. The mean ± S.D. (*bars*) of three independent experiments are shown. *C*, we cultured primary MM cells with either 10 μM K-7174 (*K-7174*) or the vehicle alone (*control*) for 48 h. Cell death/apoptosis was determined by reactivity with annexin-V on a flow cytometer. The *y* axis shows the proportion of annexin-V-positive cells (%). The values of individual samples are indicated as follows: patient 1, *open circle*; patient 3, *open triangle*; patient 4, *open diamond*; patient 5, *closed circle*; patient 7, *closed triangle*; and patient 8, *closed diamond*. *Bars* indicate the average values. *p* values were calculated by paired Student's *t* tests.

Next, we confirmed the anti-myeloma activity of K-7174 using primary MM cells. CD138-positive cells isolated from bone marrow samples of 6 patients were cultured in the absence or presence of K-7174 for 2 days, followed by annexin-V staining to assess the induction of apoptosis. K-7174 significantly increased the percentage of annexin-V-positive cells in all cases examined (Fig. 1*C*).

K-7174 Inhibits Human MM Cell Growth in a Murine Xenograft Model—Having demonstrated the cytotoxicity of K-7174 against MM cells *in vitro*, we examined the *in vivo* efficacy using a xenograft mouse model. As described previously (21), we inoculated either RPMI8226 or U266 cells subcutaneously into NOD/SCID mice in the right thigh at 3×10^7 or 1×10^7 cells. When measurable tumors developed (usually after 4 days), either K-7174 (75 mg/kg) or vehicle (3% DMSO in 0.9% NaCl) was intraperitoneally administered once daily for 14 days (n = 3–4 in each group). We compared the tumor volume between vehicle-control and K-7174-treated groups on day 14. The tumor volume was significantly lower in the K-7174-treated group than in the vehicle-control group (Fig. 2, *A* and *B*). However, the K-7174-treated group had a significant body weight reduction after 10 days (data not shown). We therefore repeated the same set of experiments with reduced doses (30 and 50 mg/kg). Although no body weight reduction was observed, K-7174 failed to inhibit tumor growth at these doses (data not shown).

As K-7174 was originally developed for oral administration, we tested the therapeutic effects of post-oral K-7174 in tumor-inoculated mice. Either K-7174 (50 mg/kg) or vehicle (3% DMSO in 0.9% NaCl) was orally administered once daily for 14 days (n = 3–4 in each group). We determined the dose of K-7174 to be well tolerated by mice without obvious side effects including weight loss in pilot experiments (data not shown). The tumor volume was compared between vehicle-control and K-7174-treated groups for up to 28 days. As a result, tumor volume was significantly lower in the K-7174-treated group than in the vehicle-control group (Fig. 2, *C* and *D*). There were no obvious side effects including body weight reduction, leukocytopenia, thrombocytopenia, anemia and hepatic dysfunction in both vehicle-control and K-7174-treated groups (the data on day 21 are shown in Table 1). To examine the proteasome inhibitory effect of K-7174 *in vivo*, we determined the accumulation of ubiquitinated proteins in inoculated tumors after oral administration of K-7174. As expected, a 2–4-fold accumulation of ubiquitinated proteins was observed in tumor cells in the K-7174-treated group but not in the vehicle-control group (Fig. 2*E*). This suggests that K-7174 could effectively inhibit proteasome activity *in vivo*. Taken together, these data demonstrate the potent anti-myeloma activity of K-7174 *in vivo* and more importantly, that oral administration is more effective than intraperitoneal injection.

K-7174 Overcomes Bortezomib Resistance in Vitro and in Vivo—Because K-7174 appears to inhibit proteasome activity with a distinct mode from bortezomib (18), it is anticipated that K-7174 is effective for bortezomib-resistant MM cells. To substantiate this notion, we have established mutant and wild-type (WT) sublines from RPMI8226 cells lentivirally transduced with mutated and wild-type PSMB5. We selected representative sublines that express the highest levels of VENUS and *PSMB5* as described previously (18). HDAC1 overexpression itself did not affect the proliferation potential and viability of myeloma cells (data not shown). Overexpression of wild-type *PSMB5* conferred modest resistance to bortezomib but not K-7174 in RPMI8226 cells. Yet, sensitivity to bortezomib was significantly lower in the mutant subline than in the WT subline in MTT assays. In striking contrast, K-7174 induced cytotoxicity equally in WT and mutant sublines (Fig. 3*A*). Next, we confirmed the activity of K-7174 against bortezomib-resistant cells *in vivo*. We inoculated either WT or the mutant subline into NOD/SCID mice as described above. When measurable tumors developed, mice were randomly assigned to 3 groups: vehicle control, 0.5 mg/kg of bortezomib treated, and 50 mg/kg of K-7174 treated groups. Bortezomib strikingly inhibited tumor growth in mice inoculated with WT subline (Fig. 3*B*, *left panel*), but failed to do so when the mutant subline was inoculated (Fig. 3*B*, *right panel*). However, K-7174 significantly retarded tumor growth in mice inocu-